

Neural substrates of accurate perception of time

duration:

A functional magnetic resonance imaging study

Hashiguchi, Maho

The Graduate University for Advanced Studies, SOKENDAI

School of Life Science

Department of Physiological Sciences

National Institute for Physiological Sciences

Department of System Neuroscience

Table of contents

1. Abstract	1
2. Introduction.....	2
3. Method	6
3.1. Participants	6
3.2. Experimental setup.....	6
3.3. Task design and stimulus preparation	7
3.4. Functional magnetic resonance imaging protocol	10
3.5. Imaging acquisition	10
3.6. Data analysis	11
3.6.1. Psychophysical data.....	11
3.6.2. Functional magnetic resonance imaging data	13
4. Results	15
4.1. Behavioral data	16
4.2. Functional magnetic resonance imaging data	18
5. Discussion	21
5.1. Unique features of the present study.....	21
5.2. The right anterior insular cortex	24
5.3. The right inferior frontal gyrus	26
5.4. Non-specificity of the right anterior insular cortex and inferior frontal gyrus in pitch discrimination.....	27
5.5. Right-lateralized neural representation of temporal discrimination	28
5.6. Psychological processing of duration discrimination tasks	29
5.7. Methodological considerations.....	30
5.8. Limitations.....	30
5.8.1. The causal relationship	30
5.8.2. Multiple duration ranges	31
5.8.3. Psychiatric disease groups	32
7. Acknowledgments	34
8. References	34
9. Supplementary Figures	46
10. Supplementary Tables	49

1. Abstract

Time duration, an essential feature of the physical world, is perceived and cognitively interpreted subjectively. While this perception is deeply connected with arousal and interoceptive signals, the underlying neural mechanisms remain elusive. As the insula is critical for integrating information from the external world with the organism's inner state, I hypothesized that it might have a central role in the perception of time duration and contribute to its estimation accuracy.

I conducted a functional magnetic resonance imaging study with 27 healthy participants performing temporal duration and pitch bisection tasks that used the same stimuli. By comparison with two referents with short and long duration in the time range of 1 s (close to the heart rate period), or low and high pitch, participants had to decide whether target stimuli were closer in duration or pitch to the referent stimuli. The temporal bisection point between short and long duration perception was obtained through a psychometric response curve analysis for each participant. The deviation between the bisection point and the average of reference stimuli durations was used as a marker of duration accuracy. Duration discrimination-specific activation, contrasted to pitch discrimination, was found in the dorsomedial prefrontal cortex, bilateral cerebellum, and right anterior insular cortex (AIC), extending to the inferior frontal gyrus (IFG), inferior parietal lobule, and frontal pole. The activity in the right AIC and IFG was positively correlated with the accuracy of duration discrimination. The right AIC is known to be related to the reproduction of duration, whereas the right IFG is involved in categorical decisions. Thus, the comparison between the referent durations reproduced in the AIC and the target duration may occur in the right IFG. I conclude that the right AIC and IFG contribute to the accurate perception of temporal duration.

2. Introduction

Time perception is central to memory, feelings, behavior, and decision-making for actions affecting the external world (Buhusi and Meck, 2005; Lane et al., 2003; Wittmann and Paulus, 2008, 2009). Within the temporal framework perceived and constructed by the brain, events seem to happen and interact (Nani et al., 2019). For example, playing an instrument requires closing the subjective time to the physical time, in other words, to an accurate perception of time duration. Thus, “Almost all our psychological processes involve time processing, and all of our actions unfold over time and rely on accurate timing” (Teghil et al., 2019). However, different from audio and visual stimuli, I do not have the receptor for temporal information. “Time has been considered an essential feature of reality, on the one hand (Unger and Smolin, 2015), or a figment of the way I know reality, on the other (Rovelli, 2018). “ (Nani et al., 2019). It is, therefore, of the utmost importance to investigate how well the subjective percept of temporal duration corresponds to its objective measure in the external world, a critical component of time perception. There is still no consensus on the mechanisms that account for the subjective sense of temporal duration (Meissner and Wittmann, 2011). An influential model incorporates the initial clock stage as an internal pacemaker producing a series of pulses and an accumulator that counts the number of pulses over a given time, which represents the duration of the experienced events (Church, 1984; Gibbon et al., 1984; Treisman et al., 1990). Fig.1 shows the internal clock model.

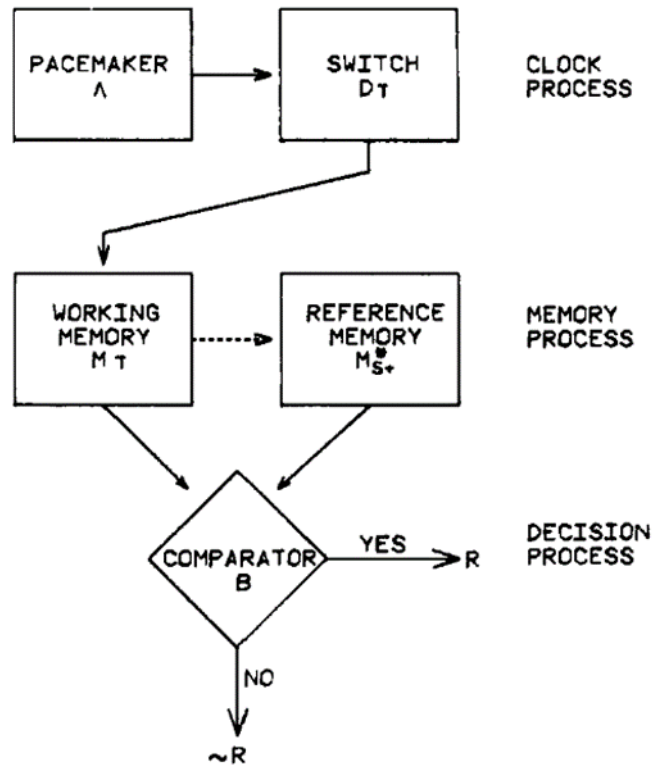


Fig.1. Internal clock model (Gibbon et al.,1984)

“Information-processing model. The top row describes a clock process with a pacemaker generating pulses switched into an accumulator for working memory (middle row). After reinforcement, working memory contents are stored in a reference memory for later comparison on subsequent trials with the current working memory value”.

Then, at the memory stage, the output of the accumulator is transiently stored in the working memory. Finally, at the decision stage, the stored duration values are compared with those in the reference memory to make decisions (Pouthas et al., 2005). In neuroscience, the neural model that assumes the striatum to be an oscillating active region is called the striatal beat-frequency model (SBF) (Matell and Meck, 2004). Several brain areas have been candidate neural substrates for perception of temporal duration, such as the frontostriatal circuits involving the supplementary motor area (SMA), right prefrontal cortex, right posterior parietal cortex, insula, putamen, and cerebellum (Buhusi and Meck, 2005; Elsinger et al., 2006; Harrington et al., 2004a; Rubia and Smith, 2004; Wittmann, 2009; Wittmann and van Wassenhove, 2009). A recent meta-analysis of functional neuroimaging studies identified the consistent involvement of the insula, pre-SMA/SMA, inferior frontal gyrus, pre-central gyrus, cingulate gyrus, superior temporal gyrus, claustrum, putamen, and caudate body (Nani et al., 2019). These areas were involved across four different categories of time processing: sub-second and supra-second timing tasks in motor or non-motor perceptual conditions. This extensive network may be activated partly by duration perception and associated cognitive demands such as memory and decision-making. By controlling cognitive demand to isolate temporal duration perception from other tasks, Livesey et al. (2007) found that the bilateral dorsal putamen, the junction of the anterior insula cortex (AIC), the inferior frontal gyrus (IFG), and the left inferior parietal cortex were crucial for temporal duration perception. In this study, I investigated the neural correlates of time duration using a temporal bisection (TB) task in a functional magnetic resonance imaging (fMRI) paradigm (Allan and Gibbon, 1991; Church and Deluty, 1977; Wearden, 1991) to behaviorally measure the accuracy of duration

perception of 1 s, which approximately corresponds to the heart rate period. This experimental task design and analysis are based on the assertion that subjective time is produced by integrating internal and external physical information (Craig, 2009b; Teghil et al., 2019). The internal information here refers to interoception such as heartbeat, and in a larger meaning that includes all subjective feelings from the body and emotional awareness (Craig, 2009b). Therefore, I hypothesized that the regions in which I integrate external physical information with internal information would be involved in the production of subjective time. In other words, it was hypothesized that there would be regions of higher activity when the integration of external physical and internal information was better, i.e., the more accurate the time duration perception. More specifically, based on an earlier report by Teghil et al. (2019), I predicted that TB task-specific activation in the insula, particularly, could be correlated across participants with the accuracy of time duration estimation.

3. Method

3.1. Participants

In total, 30 healthy, right-handed (Oldfield, 1971) individuals (15 men and 15 women; mean age \pm standard deviation, 21.8 ± 1.6 years) were included in this study. None of the participants had a history of drug exposure or neurological or psychiatric disorders. All individuals gave written informed consent for participating in this study, which our institution's ethics committee approved.

3.2. Experimental setup

The experimental task was controlled and presented by Presentation software 16.1 06.11.12 (Neurobehavioral Systems, Albany, CA, USA; RRID: SCR_002521). I presented the auditory stimuli through MRI-compatible headphones (Kiyohara Optics Inc., Japan). For each participant, the sound volume was adjusted to an appropriate level such that each participant felt that they could “comfortably” listen to the tone for task execution. The intensity level was determined before the experiment and remained unchanged during the experiment. The participant held an optical response button-box in their right hand to record their responses. Throughout the runs, the participants were asked to focus on a small, white crosshair at the center of a screen viewed through a mirror. The half-transparent viewing screen was located behind the MRI head coil, and visual cues were projected through a liquid-crystal display projector. Participants practiced the task outside the scanner for about 5 min before performing the task in the MRI scanner.

3.3. Task design and stimulus preparation

With two referents, one short and the other long, participants had to decide if the duration of a given target was closer to either referent. Based on a psychometric curve analysis, the TB task defines the bisection point (BP) as subjective equality (Allan, 2002) that represents the subjective temporal duration equidistant to both referents. Therefore, there is no “no correct or incorrect answer” in the BP position, and the TB task is appropriate for studying subjective time information processing. (Kopec and Brody,2010) .Thus, the absolute deviation of the BP determined in each participant from the arithmetic mean of the two referents was set as a quantitative marker of accuracy for duration perception (Harrington et al., 2004b). The participants performed three auditory tasks in the MRI scanner: TB, pitch bisection (PB), and motor control (C). A TB block began by presenting the visual instruction “Duration.” Each TB trial, 7.8 s in duration, presented the two pairs of auditory tones with different intervals (anchor stimuli, A1, and A2) followed by the test stimulus (T). The PB was designed to subtract from the TB to remove areas related to the cognitive load of the discrimination task. The C was to exclude activities related to pressing a button after hearing the auditory tones by subtracting the C from the PB. The first two tones comprised anchor A1 (R1-R2) and the next two tones comprised A2 (R3-R4), whereas the last two tones were the test stimuli (T5-T6). During the TB task, participants were asked, “which anchor, A1 or A2, is closer to the test stimuli T5-T6 in terms of ISI?” by presenting the visual instruction of “Duration”. Participants answered by pressing a button with either the index or middle finger of their right hand, following the visual instruction given with the terms “Short” and “Long.” After completing a block of five or six trials, the visual

instruction “Rest” appeared for 2.6 s, followed by a crosshair for 5.2 s. The PB block was identical to the TB block except for the fact that the question, “which anchor is closer to the test stimuli T5-T6 in terms of pitch?” was asked by presenting the visual instruction of “Pitch” (Fig. 2). Participants answered by pressing a button following the visual instruction given with the terms “High” and “Low” appearing side by side (Fig. 2). The C block began with the visual instruction “press either button.” Participants had to choose freely to press either the left or right button at the end of the T6 stimuli. The control trial presented a series of six random pure tones varying in ISI (817–1762 ms) and pitch (681.4–719.1 Hz). Participants randomly pressed a button without paying attention to pitch or time interval in A1 and A2. The reference stimuli R consisted of pure tones (50 ms duration with fade-in and fade-out, 10 ms each) at either 681.4 Hz (low pitch, L) or 719.1 Hz (high pitch, H). A1 and A2 were paired for each trial to differ in pitch and temporal interval. The pair R1 and R2 had the same pitch. Similarly, R3 and R4 had the same pitch. The time intervals between the stimuli within each anchor were set to 817 ms or 1762 ms. Thus, I adopted four patterns as follows:

A1	A2
High pitch Short duration	Low pitch Long duration
High pitch Long duration	Low pitch Short duration
Low pitch Long duration	High pitch Short duration
Low pitch Short duration	High pitch Long duration

The interstimulus interval (ISI) was either 850 ms, 880 ms, or 910 ms between A1 and A2 and A2 and T5. The ISI between T5 and T6 varied logarithmically between 817 ms (short anchor) and 1762 ms (long anchor) in seven steps: 817 ms, 990 ms, 1090 ms, 1200 ms, 1321 ms, 1454 ms, and 1792 ms (Fig. 2). Similarly, the pitch varied

logarithmically between 681.4 (low anchor) and 719.1 Hz (high anchor) in seven steps: 681.4 Hz, 690.6 Hz, 695.3 Hz, 700 Hz, 704.7 Hz, 709.5 Hz, and 719.1 Hz. A total of 196 trials were conducted, equally distributed between the PB and TB tasks. The details of the condition combinations are shown in Supplementary Table.1.

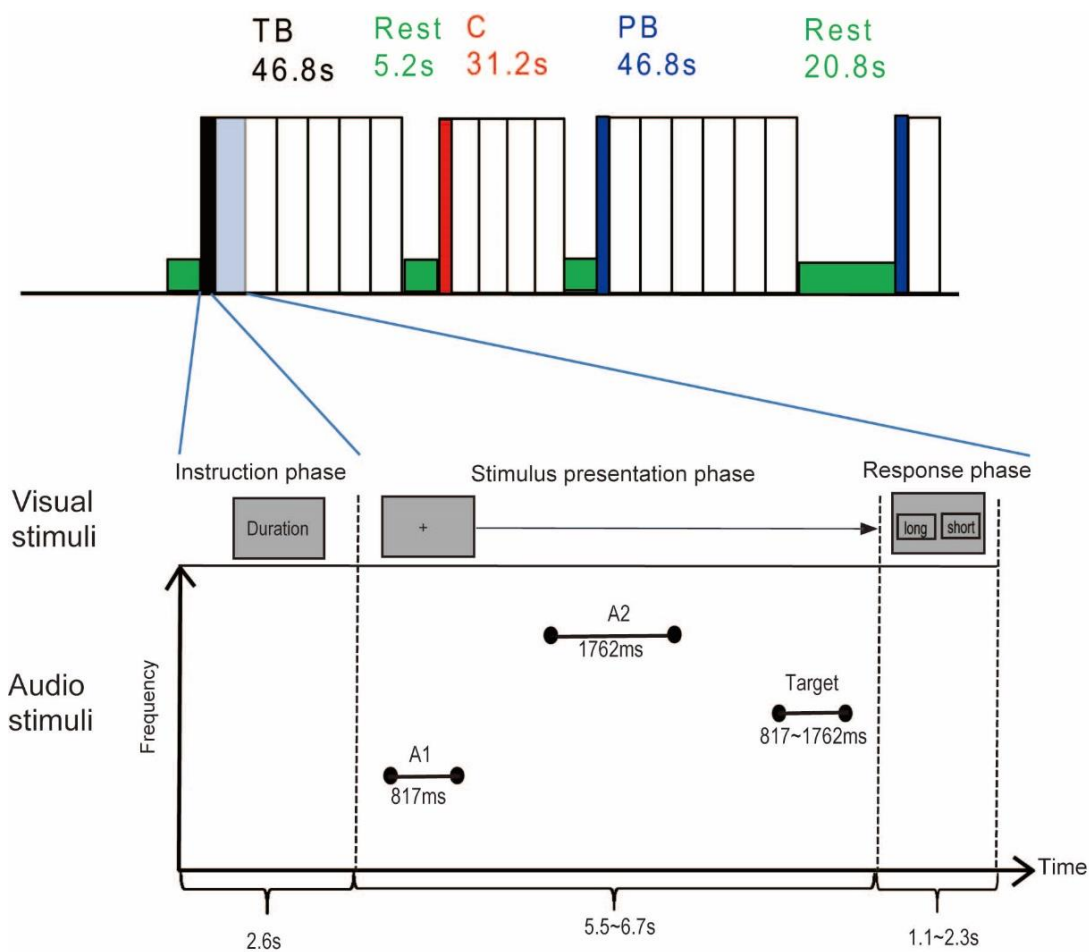


Fig. 2. Elementary task design (for runs 1, 2, and 3).

During a TB or PB trial (open rectangle), a series of six pure tones with variable intervals and pitch are presented (only four during the control trial C). One block contains six trials, and one run contains four blocks from the TB, TC, or C combinations in a random order. The interval between two blocks of different types (e.g., TB-PB) is 5.2 s but 20.8 s between

blocks of the same type (e.g., TB-TB). C, control; PB, pitch bisection; TB, temporal bisection.

3.4. Functional magnetic resonance imaging protocol

To build a balanced session, I presented identical stimuli during the PB and TB tasks utilizing 98 trials each, resulting in 196 trials to which 64 control trials were added. The 260 trials in total were organized into four runs, with the first three sharing the same structure. Each of the first three runs contained four blocks of either TB or PB, which were made of six trials each, and four blocks of the C condition containing four trials (Fig. 2). Thus, each run had 64 trials. The TB, PB, and C blocks were separated by a short rest period (5.2 s) except for consecutive blocks with the same condition (TB-TB or PB-PB), between which a long rest period (20.8 s) was inserted (Fig. 2). C conditions were never consecutive. The fourth run had a similar structure, except that it comprised five TB blocks, four of which included five trials each, and the last run included six trials; five blocks of PB with a structure identical to that of TB and four C blocks contained four trials each. This complicated design was used to sample data for the psychometric function. As two anchor stimuli were presented serially followed by the target stimulus, the order of the anchor presentation may have affected the participants' decisions. To eliminate this potential effect, the order of the two anchor stimuli was randomized.

3.5. Imaging acquisition

FMRI data were acquired using a 3.0-T head-only MRI system (Magnetom Allegra, Siemens, Erlangen, Germany). I utilized gradientecho echo-planar imaging (EPI)

sequences with the following parameters: repetition time (TR) = 2.6 s, echo time (TE) = 30 ms, flip angle (FA) = 80°, 44 axial slices, field of view (FOV) = 192 mm, matrix = 64 × 64, slice thickness = 3.5 mm with 0.47 mm gap, and voxel size = 3.0 × 3.0 × 3.47 mm. The slice order was sequentially ascending. The number of volumes obtained per run was 253 for run 1–3 and 277 for run 4. I obtained high-resolution structural whole-brain images using a T1-weighted magnetization-prepared rapid-acquisition gradient echo (MP-RAGE) imaging sequence with the following parameters: TR = 2600 ms, TE = 4.38 ms, FA = 8°, FOV = 256 mm, matrix = 256 × 256, 192 slices, and voxel size = 1.0 × 1.0 × 1.0 mm.

3.6. Data analysis

Data are presented as the mean ± standard error of the mean.

3.6.1. Psychophysical data

I calculated the judgment probability (p) for each test condition task. In the TB task, p was defined by reference to the long anchor. The psychometric variables k and t_0 were determined using the logit function of Eq. (1):

$$p = \frac{1}{1 + e^{-k(t-t_0)}} \quad , \quad (1)$$

where t is the length of the test stimulus, t_0 is the threshold (the length of the stimulus time such that the probability of answering “closer to the long duration” is the same as the probability of answering “closer to the short duration”), and p is the probability of answering “closer to the long duration.” Thus, t_0 represents the subjective temporal

duration equidistant to the anchor durations. Using Eq. (1), I performed a linear regression analysis on the experimental data (data at seven points), where the slope at t_0 becomes steeper as k increases.

Thus, k reflects the sensitivity or precision to time perception differences, which has been termed the Weber ratio (WR) (Kopec and Brody, 2010). The parameter t_0 is the BP. When BP deviates to the left of the arithmetic mean of the long and short duration reference stimuli (i.e., when it is small), there is a bias toward a perception of long durations, whereas when BP is higher than the mean of the reference stimuli durations, there is a bias toward the perception of short durations. Therefore, the distance of BP from the arithmetic average of the two standard stimuli provides an estimate of the accuracy for the estimation of the given time interval. To check if there is a systematic effect of the order on the BP estimation, I obtained psychometric functions separately from trials in which anchors were presented in the order of short (817 ms) to long (1762 ms) duration and from trials in the reverse order. I calculated the difference between the BP of different orders of anchor presentation, a positive value indicating a primacy effect, whereas a negative one indicates a recency effect. This procedure aimed to check the “subjective shortening” of past durations which is usually observed for durations exceeding 3 s (Wackermann and Spati, 2006). I performed an identical analysis on the PB data, in which the probability was determined as to how close a participant’s judgment was to the high-pitch anchor. Similar to the TB condition, I acquired the precision (WR) and accuracy (BP) of pitch discrimination.

As the accuracy of time duration may differ across genders (Block et al., 2000), I have checked gender differences in psychological quantities, WR, reaction time, and BP in the TB and PB tasks, and absolute T_0 and P_0 by splitting the dataset into two subgroups: the

male group (N=13) and the female group (N=14). The Man-Whitney U test tested the group difference.

3.6.2. Functional magnetic resonance imaging data

3.6.2.1. Preprocessing

The first two volumes from each fMRI acquisition were discarded because of unstable magnetization, and the remaining 520 vol (248 for runs 1–3 and 272 for run 4) were used for the analysis. I preprocessed the data using the SPM8 software (Wellcome Trust Centre for Neuroimaging, London, UK) implemented in MATLAB (MathWorks, Natick, MA, USA). The EPI images were first realigned for motion correction, then coregistered with the whole-head MP-RAGE image volume. They were then normalized to the Montreal Neurological Institute (MNI) stereotaxic space and smoothed with an isotropic Gaussian kernel of 8-mm full-width-at-half-maximum in the x, y, and z axes.

3.6.2.2. Statistical analysis

I used SPM12 for statistical analyses with the general linear model. The task-related regressors of the TB block, PB block, and C block were implemented as regressors of interest. The duration of each block was set from the first trial to the last one. I also included instruction, button press, and motion regressors as covariates of no-interest in addition to these three regressors. The high-pass filter was set to “infinity,” and the global normalization setting was “scaling.” I adopted the AR (1) model to create a correction for autocorrelation. At this individual-level analysis, I used (TB > C) and (PB > C) contrasts to depict the neural basis of TB and PB tasks, respectively. These two contrast images were then used in a second-level (group) analysis. For the group-level analysis, I first used the one-sample t-test to retrieve the neural substrates of TB and

PB, respectively. Second, to highlight the neural substrates that are specifically associated with the TB task, I used the paired t-test from the (TB > C) and (PB > C) contrast maps. Using the inclusive mask in SPM, I confined the search area within the region, which shows statistically significant activation in the one-sample t-test with (TB > C) contrast maps. Third, to test our main hypothesis on whether any brain region is correlated with TB variance, I used the one-sample t-test with covariates. Two psychophysical quantities, slope WR and BP of the TB task, T_{abs} , for the TB tasks, were included as covariates in this one-sample t-test analysis. A similar procedure was applied to the PB task. Through this analysis, I could test whether there are any regions in which brain activation is correlated with T_{abs} or slope in the TB or PB conditions. I limited the search region to the area that showed greater activation in TB. In this covariate analysis, the statistical significance was adjusted by using a small volume correction. In these group-level analyses, the statistical threshold was set at $p < .05$ (family-wise error-corrected) at the cluster level (Friston et al., 1996) with a height threshold of $p < .001$ (uncorrected) at the voxel level (Flandin et al., 2019). The anatomical locations were determined using the SPM Anatomy Toolbox (Eickhoff et al., 2005, 2006, 2007), and I confirmed the locations using a printed atlas (Mai et al., 2015). I also used MRICroN (<https://people.cas.sc.edu/rorden/mricron/index.html>) to overlay regions that describe (TB > C) and (PB > C).

While the gender of participants who participated in the present experiment was well balanced (male =13, female = 14), it is possible that task-related activation shows a gender-specific effect. To test the possibilities, I compared brain activation related to the TB task. The comparison was made on a second-level analysis. I separated participants into two groups, male (N = 13) and female group (N = 14), and

tested whether or not the task-related activation differs between groups by using a two-sample t-test.

The GLM analysis introduced in the present study could evaluate the brain activation that is activated/deactivated specifically in the TB task and could illustrate the regions associated with the accuracy of the TB task. However, there is another possibility that the functional connectivity involving some brain regions is enhanced/decreased specifically by the TB task and is correlated to the accuracy of the TB task, while the activation in the region does not show a task-related effect. I introduced the psycho-physio-interaction (PPI) analysis with the CONN toolbox (<http://www.nitrc.org/projects/conn>) to test this possibility. As regions of interest (ROIs), I selected six regions of the right AIC, the IFG, the middle frontal gyrus (MFG), the inferior parietal lobule (IPL), the bilateral cerebellum, and the medial prefrontal cortex: Six regions were specifically activated in the TB condition (See, Fig. 4), and two regions of the right AIC and right IFG were related to the accuracy of duration perception (See, Fig. 5). Among these ROIs, I tested whether the ROI-to-ROI functional connectivity was influenced more in the TB condition than PB condition and whether the differences of functional connectivity between TB and PB (TB>PB) was correlated with the accuracy of time duration perception. The statistical threshold was set to $p < 0.05$ at a group level (FDR corrected), which is a default threshold in CONN toolbox.

4. Results

Data from one participant were lost due to problems with our MRI scanner. Moreover, two participants had to be excluded due to poor performance. I included participants for whom the proportion of incorrect responses to the shortest duration was lower than 3

standard deviations. The standard deviation for incorrect responses from those participants for the 817-ms duration discrimination was above this threshold (0.43 and 0.50, respectively [mean = 0.07, standard deviation = 0.12]). Thus, 27 participants (13 male and 14 female) were considered for the analysis.

4.1. Behavioral data

In the TB task, the BP was 1271.06 ± 21.30 ms, and the Weber ratio was 0.010 ± 0.0008 . The absolute deviation of BP from the arithmetic average of the two standard stimuli, i.e., the distance from the median point, was 80.74 ± 15.0 ms. As one participant showed that during short duration first condition the BP was out of range (1863 ms), I tested the anchor order effect with 26 participants. The BP with anchor presentation of short (817 ms) duration first was 1237.11 ± 20.03 ms and that with anchor presentation of long (1762 ms) duration first was not significantly different with a value of $1269.20 \text{ ms} \pm 19.08$ ($N = 26$, $p = .136$, Wilcoxon signed-rank test). Thus, in this study, the effect of the anchor order was negligible. In the PB task, the BP was 700.99 ± 0.84 Hz, and the Weber Ratio was 0.26 ± 0.03 . The distance from the median point was 3.22 ± 0.59 Hz.

There were no gender differences in the WR of the TB task ($p=.061$), WR of the PB task ($p=.616$), the reaction time of the TB task ($p=.402$), the reaction time of PB task ($p=.616$), absolute of T0 ($p=.519$) or absolute of P0 ($p=.905$) (All of these tests used the Mann-Whitney U test.). In the TB task, there was a significant difference in the bisection point between the two groups ($p=.014$, Mann-Whitney U test). Female participants ($N=14$) tended to estimate the temporal duration longer (1226.8 ± 24.29 ms)

compared to the male participants (1318.7 ± 30.59 ms). In the PB task, the bisection point difference between groups was insignificant ($p = .068$, Mann-Whitney U test).

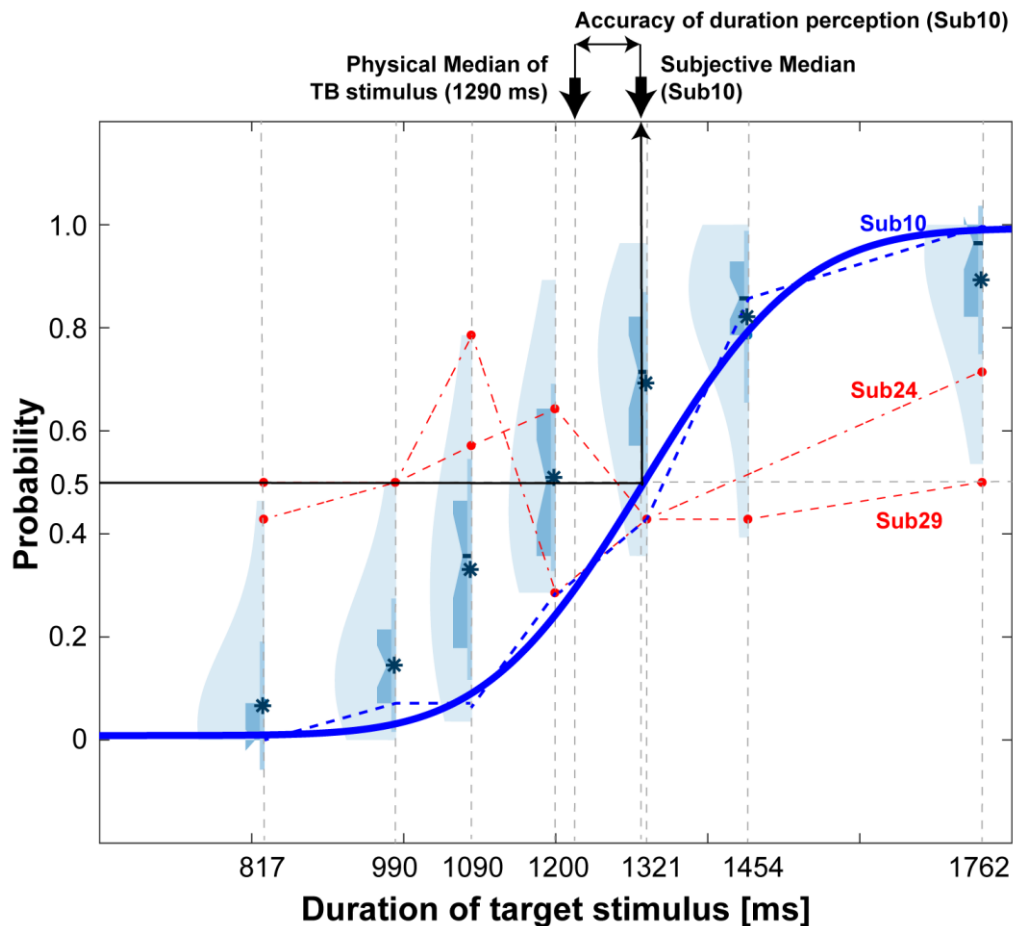


Fig. 3. Psychometric function of the judgment probability responding with “long” in the temporal bisection task.

The bisection point is defined as the duration which produces 50% “long” responses.

The accuracy of duration perception is defined as the absolute distance of the bisection point from the arithmetic average of the durations of the two anchor stimuli (1290 ms). The proportion of long responses per test duration is depicted with an average value (asterisk). Light blue areas indicate the distribution between the 99th

percentile and 1st percentile, and dark blue zones with notches between the 3rd quantile and 1st quantile with horizontal bars indicate the median. Dark blue sticks indicate the range of mean \pm standard deviation. Typical individual data (Sub10, in blue) with a fitting curve utilizing the logit function (formula (1)) was shown. Two participants (shown in red) were excluded due to poor performance.

4.2. Functional magnetic resonance imaging data

Among all areas that were activated in the TB task more than under the control, C, conditions (TB > C), the TB task induced a stronger activation compared to the PB task (TB > PB) in the right AIC, the IFG, the middle frontal gyrus (MFG), the inferior parietal lobule (IPL), the bilateral cerebellum, and the medial prefrontal cortex (Fig.4). The table corresponding to Fig. 4 is shown in Supplementary Table.2 TB-specific activation, identified by (TB > C), in the right AIC and right IFG has negatively correlated with the absolute deviation of BP from the arithmetic mean of the reference durations (the distance from the median point; Fig. 5). The table corresponding to Fig. 5 is shown in Supplementary Table.3 The activation of these areas did not correlate with WR, which represents sensitivity. Furthermore, the PB-related activity did not show a significant correlation with the distance of the BP from the median point in the PB task ($p = .86$ in the right AIC, $p = .145$ in the right IFG; Fig. 6).

I tested whether the correlation between the accuracy of TB task and TB-related activation in the AIC and IFG (Fig. 5) is influenced by gender of participant. The group analysis with two-sample t-test showed that the gender effect is only in the right occipital cortex including the cuneus (Data now shown), confirming that the activation

in the IFG associated with the accuracy of TB task has no relation to participants' gender.

The ROI-to-ROI PPI analysis showed that the TB-specific functional connectivity (TB>PB) between the right AIC and MFG was positively significantly correlated with the accuracy of TB task (FDR corrected $p < 0.05$).

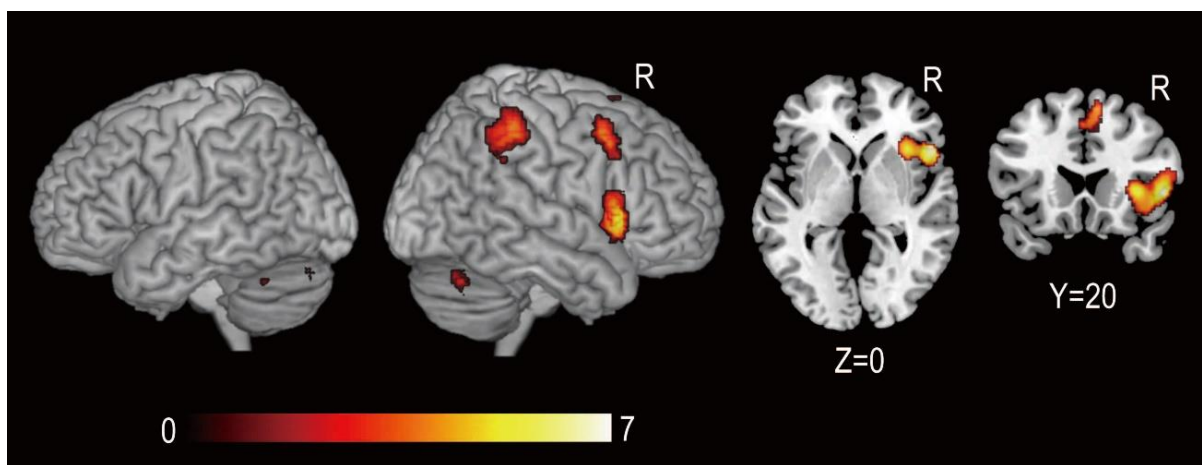


Fig.4. Temporal Bisection task-specific activity.

The contrast was (TB > PB) masked by (TB > C) depicting brain regions that are more active during the TB task than the PB task. The statistical threshold was set at $p < .05$, family-wise error-corrected at cluster level using the height threshold of uncorrected $p < .001$, within the volume defined by (TB > C). The color scale indicates t values. C, control; PB, pitch bisection; TB, temporal bisection.

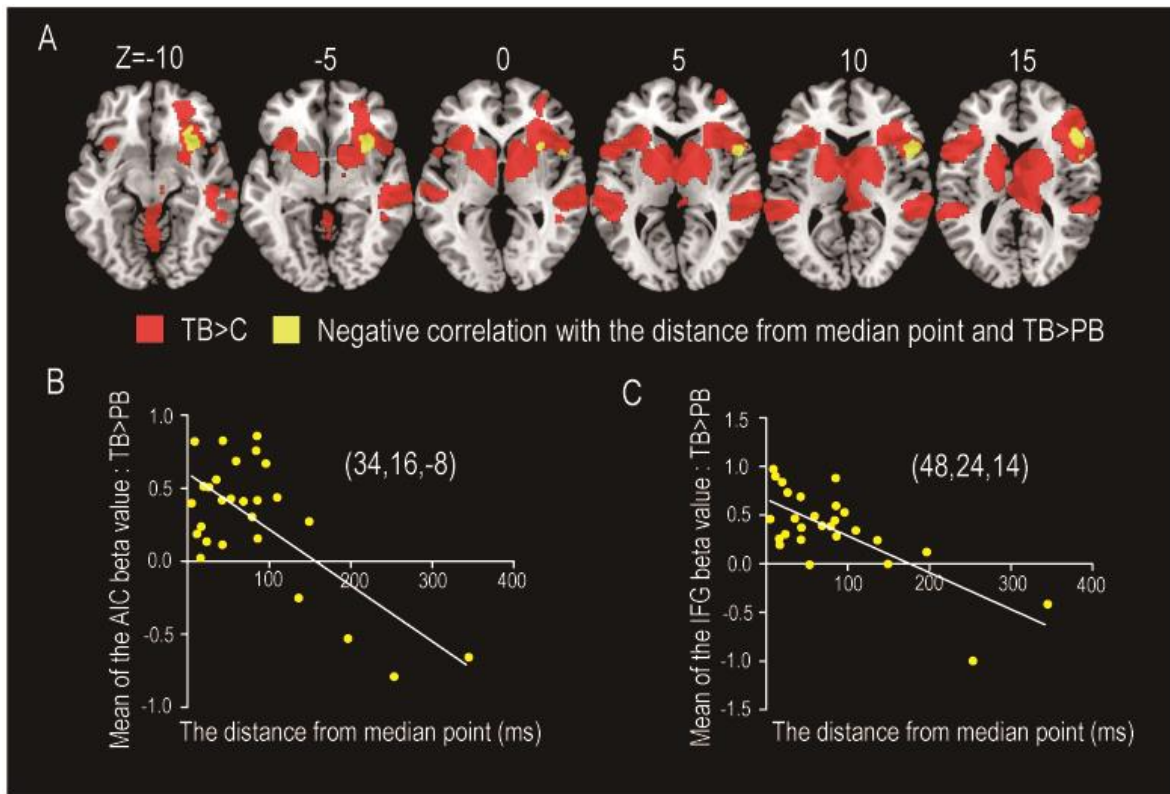


Fig. 5. Neural substrates of subjective time perception.

(A) Red indicates the areas with TB-specific activation defined by stronger activation in the TB task compared to C conditions (TB > C). Yellow indicates the area with TB-specific activation, negatively correlated with the distance of the bisection point from the median point. (B) TB-specific activation (TB > PB) in the right AIC, and (C) the right IFG (C), are plotted against the distance from the median point. AIC, anterior insular cortex; C, control; IFG, inferior frontal gyrus; PB, pitch bisection; TB, temporal bisection.

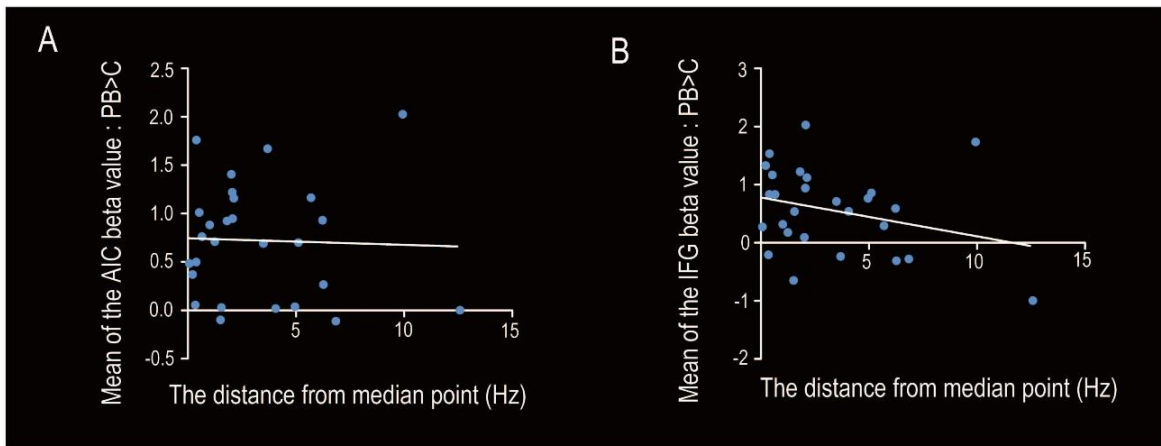


Fig. 6. Non-specific activation of the right AIC and IFG by pitch discrimination.

The pitch discrimination-related activation (PB > C) of the right AIC (A) and right IFG (B) does not show a significant correlation with the distance of the bisection point in the PB task from the median point ($p = .86$ and $.145$, respectively). AIC, anterior insular cortex; C, control; IFG, inferior frontal gyrus; PB, pitch bisection.

5. Discussion

The present study showed that the activity in the right AIC and IFG during temporal duration discrimination tasks was positively correlated with the accuracy of the duration estimation.

5.1. Unique features of the present study

The association between neural activation and standard psychological measures of time duration markers, such as BP, has been previously explored by neuroimaging studies. Harrington et al. (2004a) found that the temporal interval encoding-related activation in the right parahippocampus and hippocampus is positively correlated with the BP. They suggest that the medial temporal lobe activity represents the memory

output from an internal clock. Tipples et al. (2013) conducted both a TB task and a control task (sex discrimination task). They hypothesized that the SMA, as the internal clock, is responsible for accumulating units of time. Thus, its task-related activity should be correlated with the subjective perception of temporal duration measured by the BP. They found increased activation of the right SMA, pre-SMA, and basal ganglia. The negative correlation of BP with the TB task-specific activation contrasted with their simultaneous activation in the right SMA, pre-SMA, and IFG in the sex discrimination task. As a larger BP indicates a shorter perceived time interval, Tipples et al. (2013) concluded that these areas are related to the accumulation of a number of units of time, that is, the clock stage (Pouthas et al., 2005). The present study differs from that by Tipples et al. (2013) with respect to two points. First, I was interested to determine how the subjective perception of duration represented by BP was matched with the actual measure of duration in the physical world. I chose to utilize BP as a measure of duration perception accuracy by calculating the distance of each participant's BP from the median point between the short and long referents. Second, I hypothesized that the AIC-mediated interoceptive process affects the accuracy of time perception because of its integrative function, as suggested by Craig's model (Craig, 2009b). The AIC is of particular interest considering the subjective characteristics of temporal duration perception. To account for the complex interplay between endogenous and exogeneous factors in temporal processing, Teghil et al. (2019) postulated two complementary, yet distinct, timing mechanisms: an internally-based timing mechanism (IBT), which mediates the generation of temporal representations independently from the sensory environment, and an externally-cued timing mechanism (ECT), which primarily operates when temporal representations are based on exogenous inputs.

They suggested that ECT involves the detection of environmental temporal regularities and their integration with the output of IBT processing to generate a representation of time that reflects the temporal metric of the environment. Using ALE meta-analysis of fMRI studies, Teghil et al. (2019) found that both IBT and ECT tasks commonly activate the SMA, IFG, and right basal ganglion, while ECT tasks recruit additional areas, including the posterior cingulate gyrus, posterior superior temporal gyrus, and bilateral insula. As the bilateral anterior insula was also activated by IBT, the authors suggested that the AIC represents an endogenous temporal index (Craig, 2009a). According to Craig's model (Craig, 2009a), salient activity integration relies on an accumulation function of physiological changes in the posterior insula (Wittmann et al., 2010), which is then processed in a posterior-to-anterior progression (Craig, 2009b; Nani et al., 2019; Singer et al., 2009). The AIC integrates information from the external world and within the organism to produce a "global emotional moment," representing the sentient self at one moment. The kinematic change of this "global emotional moment" is the basis of our inner experience of duration (Craig, 2009b). In other words, "when salient moments occur rapidly, the number of global emotional moments increases during that time and, as a consequence, subjective duration dilates" (Craig, 2009b). Thus, the subjectivity may originate from processes of interoceptive bodily information (Craig, 2009a, 2009b). Simultaneously, correspondence of subjective time perception to reality is likely mediated in the insula in which the integration with information from the external world occurs. Based on this notion, Meissner and Wittmann (2011) reasoned that if "the flow of interoceptive signals from the body is essential for the representation of duration," then individuals with a high degree of interoceptive awareness, sensitively perceiving bodily changes such as pulse rates, should perform more accurately in time

estimation tasks. These authors found that individuals with better accuracy at estimating their heart rate are also better estimators of a given temporal duration during repeated temporal reproduction trials in the range of 8–20 s. Furthermore, a recent neuropsychological study in patients with an insular lesion indicated a specific role of the right insula in the discrimination of duration (Mella et al., 2019). However, the functional role of the AIC in the accurate estimation of temporal duration is unclear. The present study showed that the TB-specific activation of the right AIC and IFG, revealed by the (TB > PB) contrast, was positively correlated with the accuracy measured by the deviation of the BP from the median point of the two referents. The activation of these areas did not correlate with the WR, which represents the sensitivity. This finding is consistent with the notion that these areas are involved in the integration of ECT and IBT for promoting the accuracy of temporal discrimination.

5.2. The right anterior insular cortex

A previous meta-analysis of neuroimaging studies showed that the AIC is involved in the motoric and perceptual temporal processing of both sub-second and second ranges (Nani et al., 2019). The anterior insula is known to have several basic mechanisms: “(1) bottom-up saliency detection, (2) switching between other large-scale networks to facilitate access to attention and working memory when a salient event occurs in both internal and external environments, (3) interaction of the anterior and posterior insula to modulate physiological reactivity to salient stimuli, and (4) access to the motor system via strongly coupling with the anterior cingulate cortex” (Menon and Uddin, 2010). These mechanisms are feasible for the integration of information from the external world with the subjective time percept that originates from

interoceptive bodily information. In primates, the insular cortex integrates multiple signals of both external and internal origins, and it primarily functions as an interoceptive cortex, that is, sensing the entire body's physiological conditions (Wittmann, 2013). In the human insular cortex, sequential body states with cognitive and motivational needs are integrated through a posterior-to-anterior representation progression (Wittmann, 2013). Functional neuroimaging studies in humans showed that encoding of 9-s durations caused climbing neural activity in the posterior insula, and its reproduction caused climbing neural activity in the anterior insula (Wittmann et al., 2010). Thus, this accumulated activity with a posterior-to-anterior gradient may be related to the encoding and reproduction of the cumulative representation of time (Wittmann, 2013). This study revealed the involvement of the anterior insula in temporal duration discrimination within the range of 1 s. The previous lesion studies of the right insula indicated its functional relevance in time perception. Monfort et al. (2014) reported a case study of a patient with a focal lesion in the right anterior insula, showing global overestimation of duration during a temporal reproduction task in the supra-second range, thus, reduced accuracy, while the precision was preserved. They concluded that the representation of duration length involved the right AIC/IFG (Monfort et al., 2014). Recently, Mella et al. (2019) reported 21 patients with strokes affecting the insula. They found that patients with a right insular lesion showed less temporal sensitivity than both control participants and patients with left insular lesions. As the extent of the lesion covered mainly the posterior region, Mella et al. (2019) suggest that the posterior part is involved in the encoding of duration, while the anterior insula participates in the reproduction of intervals (Wittmann et al., 2010). Finally, the TB-specific functional connectivity (TB>PB) of the right AIC with MFG was positively

correlated with the accuracy of TB task. As the right MFG showed the TB specific activity, this finding confirms the integrative role of the right AIC in the integration of external physical and internal temporal information. The current findings indicate that the anterior portion of the insula is related to the accuracy of temporal discrimination, consistent with its integrative function with respect to information from both internal and external environments (Craig, 2009b).

5.3. The right inferior frontal gyrus

By contrast, the right IFG is related to categorical decisions (Cromer et al., 2010; Jiang et al., 2007). The right IFG is involved in the duration discrimination task that requires working memory function to allow comparison across two intervals (Hayashi et al., 2013; Mottaghy et al., 2003). Hayashi et al. showed that the right IFG is related to more-versus-less categorical information irrespective of the domain of time and numerosity. Specifically, they found that transcranial magnetic stimulation of the right IFG interferes with categorical duration discrimination, whereas that of the right inferior parietal cortex modulates the influence of numerosity on time perception. They concluded that the right IFG is specifically involved in the categorical decision stage. Therefore, the right IFG in the present task is likely involved in the decision phase, in which the comparison between the referent durations reproduced in the AIC and the target duration took place.

5.4. Non-specificity of the right anterior insular cortex and inferior frontal gyrus in pitch discrimination

Although PB-related activity in the right AIC and IFG was not significantly correlated with the distance of the BP in the PB task from the median point, these brain regions showed PB-related activity. This may be explained by the common psychological processes in the perceptual discrimination task, that is, selective attention and categorical decision. The AIC is related to the selective attention toward different characteristics of an object (Yoshioka et al., 2021). In the present study, participants had to attend to the different features of a given stimulus, that is, temporal duration or pitch. These task sets led to the general activation of the right AIC. The right IFG is related to categorical decision-making irrespective of the features of the object.

Previous non-human primate studies revealed that the prefrontal cortices are involved in decisions based on both spatial and temporal information (Genovesio et al., 2011) and episodic memory (Genovesio et al., 2009). Thus, both temporal and pitch discrimination tasks recruited the right AIC for selective attention and the right IFG for categorical decisions. The difference in the difficulty of the two tasks may have influenced the non-specificity of the activities of the right AIC and IFG for the PB. To test this issue, I compared the median reaction time between the two tasks. The median reaction time of the TB task was 853.10 ± 22.65 ms and that of the PB task was significantly different with a value of 709.87 ± 29.02 ms ($N = 27$, $p < .001$, Paired t-test). However, there were no activation areas that correlated with the difference in median reaction time for the TB and PB tasks. Therefore, although the difficulty of the two tasks might not be the same controlled, the activities of right AIC and IFG related to the accuracy of duration perception depicted in this study do not reflect the difference in

reaction time between the two tasks. In the design of this auditory task, the participant was able to make comparisons with the anchor as soon as he heard tone 5 before tone 6 when performing the PB task. Therefore, I think that the participants were able to make discrimination decisions faster in the PB task than in the TB task and that there was a difference in the reaction time between the two tasks.

5.5. Right-lateralized neural representation of temporal discrimination

The (TB > PB) contrast demonstrated right-lateralized activation, which is consistent with the general notion that temporal processing is preferentially right-lateralized (Ferrandez et al., 2003; Mella et al., 2019; Pouthas et al., 2005). The right IPL and IFG are both parts of the magnitude system (Hayashi et al., 2013). The magnitude system handles both time and numerosity. Hayashi et al. (2013) found that the right IPL is related to the numerosity-time interaction at the perceptual level. By contrast, the right IFG is specifically related to categorical decisions suggesting a two-stage model of numerosity-time interactions. Previously, such a system has been indicated as the "A Theory of magnitude (ATOM)," and the right IPL has been considered to be the region that contributes to the commonality of time, space, and quantity processing (Walsh et al., 2003). In addition, left hemispatial neglect caused by damage to the right hemisphere including the right parietal region is attributed to impairment of the right hemisphere-lateralized attentional network (Corbetta and Shulman, 2011). Moreover, such patients who cannot perceive and respond to unilateral space show disability in the temporal dynamics of milliseconds to a few seconds and neglect the past and future of the stimulus as well (Becchio and Bertone, 2006). Therefore, I think that the

right-lateralized temporal discrimination reflects attention to the physical information of time, space, and quantity.

5.6. Psychological processing of duration discrimination tasks

The behavioral analysis indicated that the participants conducted both TB and PB tasks successfully. The TB task requires estimating the duration of the stimuli, storing duration information in the memory, recalling such memories, and comparing two durations (Kopec and Brody, 2010). To control for these memory processes, I adopted a PB task (Harrington et al., 2010) which shares the procedure and the stimuli of the TB task, except for the instruction that specifies the features of the paired auditory stimuli, duration or pitch, to be compared. Hence, I expected the involvement of selective attention, working memory, and decision-making to be controlled.

A conjunction analysis revealed that the cerebellum, midbrain, striatum, pre-SMA, bilateral frontoparietal network, dorsolateral prefrontal cortex, and anterior insula were also activated in agreement with the involvement of those neural substrates with the abovementioned psychological processes. Three figures and two tables are shown in the supplementary as the step that discussed such psychological processes. First, Supplementary Figure 1 and Supplementary Table 4 show the areas described by TB > C. These areas contain psychological processes that are common to the PB and TB tasks. Therefore, I subtracted the PB > C activations shown in Supplementary Figure 2 and Supplementary Table 5 from TB > C. The commonality of the psychological processes of the TB and PB tasks was considered based on the commonality of the activation areas shown in Supplementary Figure 3.

5.7. Methodological considerations

It is crucial to control for the subject's ability to use counting as a strategy to keep track of time during time-estimation tasks. Chronometric counting, a language-based method using inner speech, supports more precise estimates than the interval-timing system and is also guided by different brain structures, particularly in the range of >10 s (Hinton et al., 2004). The present study, thus, focused on intervals around 1 s to minimize any influence of this counting effect. The arousal level is an essential factor influencing task performance. The stimulus intensity is also a factor to be considered in this regard. In the present study, I postulated that a sound that was too loud or too soft would affect the arousal level. Thus, I adjusted the intensity of the heard sound such that each participant felt that they could "comfortably" listen to the tone. The intensity level was determined before the experiment and unchanged during the experiment. In addition to the sound intensity, the individual difference in attentional focus is a confounding factor. Some participants may pay more attention to the first anchor (primacy effect) and others to the second one (recency effect). To eliminate this confounding factor, I have checked the order of anchor presentation effect on BP, which was not significant. Approximately half the participants showed the primacy effect, whereas the other half showed the recency effect; thus, this effect was well balanced across the participants. As I adopted a counter-balanced presentation of the anchors, the overall impact of attention was canceled individually.

5.8. Limitations

5.8.1. The causal relationship

Although I found a correlational relationship between the activity within the right AIC and IFG with the degree of accuracy of duration, I could not establish any proof of a

causal relationship. A future study with the use of transcranial magnetic stimulation (TMS) /transcranial direct current stimulation (tDCS) is warranted. However, TMS for AIC is technically difficult, and the safety of stimulating AICs with low-frequency repetitive TMS (1 Hz) using Heschl coils (H coils) was confirmed, but no effects on behavioral markers were observed (Spagnolo et al.,2019). Recently, the causal relationship between the structural connections between the anterior putamen and the right anterior part of the inferior frontal cortex and performance has been reported using ultrasound stimulation (Nakajima et al.,2022). In the future, I may be able to investigate the causal relationship between right AIC, IFG activity, and accuracy of duration perception by using such a stimulation technique for deep brain structure. A previous study that examined the causal relationship between the IFG and MFG connectivity and multimodal information processing found a decrease in task performance to integrate language and gesture by TMS over the IFG (Zhao et al.,2021). Furthermore, the dynamic interaction between frontal control regions and temporal representation regions might contribute to multimodal information integration (Zhao et al.,2021).

5.8.2. Multiple duration ranges

While the present study highlights the involvement of the right AIC and IFG in the accuracy of time duration perception, the current study only investigated the time duration range of 1-2 seconds. Traditionally, it has been believed that temporal information processing relies on different neural dynamics in sub-second and supra-second ranges (Coull et al., 2011). Subcortical structures may contribute to temporal information processing in sub-second ranges, and cortical areas contribute to

processing in supra-second ranges (Nani et al.,2019). However, common regions that do not depend on duration range have also been identified. The insula is particularly emphasized as an essential region that accumulates physiological changes and forms the basis for subjective time (Nani et al.,2019; Craig,2009a,2009b). The processing of body information in the right AIC spans from supra-second to multiple-second ranges (Craig, 2009a,2009b; Wittman et al.,2010). Previous studies also found associations between timing accuracy from 2 to 24 seconds and vagal control (Pollatos et al.,2014) and duration reproduction accuracy at 8, 14, and 20 seconds with cardiac awareness (Meissner and Wittman,2010). Based on these findings, it is suggested that the temporal duration range requiring the integration of internal and external information is from sub-seconds to around 20 seconds. Therefore, the accuracy of duration perception within this range is expected to be related to the right AIC and IFG, as seen in the present results. However, it is essential to ensure that participants do not engage in counting during time perception tasks longer than 2 seconds. Further research is needed to determine if similar neural correlates are present for shorter or longer duration ranges.

5.8.3. Psychiatric disease groups

Finally, I identified the neural substrates for the accuracy of temporal discrimination in healthy adults. The application of the experimental design to participants experiencing psychiatric disorders would be of high interest. Deficits in time perception have been observed in impulsive disorders, such as impulsive borderline personality disorder (Berlin and Rolls, 2004), stimulant dependency (Wittmann et al., 2007), and attention-deficit/hyperactivity disorder (Rubia et al., 2009). These findings imply an association

between impulsiveness and a time perception deficit (Barkley et al., 2001; Plichta et al., 2009; Rubia et al., 2009). Similarly, patients with schizophrenia show deficits in duration discrimination (Davalos et al., 2002; Elvevåg et al., 2003), and patients with depression perceive a slowing of the pace of time (Blewett, 1992; Bschor et al., 2004). Thus, depicting the neural underpinning of time processing contributes to the understanding of psychiatric disorders. To better understand their pathophysiology, future studies in patients examined using the present task design are warranted. For example, it was known that the bilateral insula is activated in fMRI measurements of schizophrenia patients during auditory hallucinations (Sommer et al., 2008). Furthermore, there are suggestions that abnormalities in AIC saliency detection and connectivity with other regions may contribute to psychiatric disorders such as schizophrenia and anxiety disorders (Menon and Uddin, 2010). I expect a decrease in the accuracy of duration perception in patients with psychiatric symptoms that cause AIC activation, such as auditory hallucinations.

6. Conclusion

Using functional MRI with healthy volunteers, I found that the right AIC and adjacent IFG, along with other cortical and subcortical regions, contribute to the accuracy of duration perception. The human AIC, along with the anterior cingulate cortex, is one of the most commonly affected regions in psychiatric disorders (Goodkind et al., 2015; Nagai et al., 2007; Seeley, 2008) which often manifest deficits in temporal processing. Further studies in psychiatric patients examined with the present task design are warranted.

7. Acknowledgments

First of all, I would like to express my deepest gratitude to Dr. Norihiro Sadato for his guidance and support for this dissertation. I would also like to thank Dr. Takahiko Koike, Dr. Tomoyo Morita, Dr. Tokiko Harada, and Dr. Denis Le Bihan for their invaluable assistance with this thesis. I am also deeply grateful to Dr. Shuntaro Okazaki for his great suggestions in conceiving this experimental task design. I am also grateful to the technical and administrative staff of the Systems Neuroscience Division of NIPS for their kind support. Finally, I would like to express my deepest gratitude to all the people who have supported this research.

8. References

- Allen, M., Fardo, F., Dietz, M.J., Hillebrandt, H., Friston, K.J., Rees, G., Roepstorff, A., 2016. Anterior insula coordinates hierarchical processing of tactile mismatch responses. *Neuroimage* 127, 34–43. <https://doi.org/10.1016/j.neuroimage.2015.11.030>
- Allan, L.G., Gibbon, J., 1991. Human bisection at the geometric mean. *Learn. Motiv.* 22, 39–58. [https://doi.org/10.1016/0023-9690\(91\)90016-2](https://doi.org/10.1016/0023-9690(91)90016-2)
- Barkley, R.A., Murphy, K.R., Bush, T., 2001. Time perception and reproduction in young adults with attention deficit hyperactivity disorder. *Neuropsychology* 15, 351–360. <https://doi.org/10.1037/0894-4105.15.3.351>
- Becchio, C., Bertone, C., 2006. Time and neglect: Abnormal temporal dynamics in unilateral spatial neglect. *Neuropsychologia* 44, 2775–2782. <https://doi.org/10.1016/j.neuropsychologia.2006.06.011>

- Berlin, H.A., Rolls, E.T., 2004. Time perception, impulsivity, emotionality, and personality in self-harming borderline personality disorder patients. *J. Pers. Disord.* 18, 358–378. <https://doi.org/10.1521/pedi.2004.18.4.358>
- Blewett, A.E., 1992. Abnormal subjective time experience in depression. *Br. J. Psychiatry* 161, 195–200. <https://doi.org/10.1192/bjp.161.2.195>
- Block, R.A., Hancock, P.A., Zakay, D., 2000. Sex differences in duration judgments: A meta-analytic review. *Mem. Cogn.* 28, 1333–1346. <https://doi.org/10.3758/BF03211834>
- Bschor, T., Ising, M., Bauer, M., Lewitzka, U., Skerstuveit, M., Müller-Oerlinghausen, B., Baethge, C., 2004. Time experience and time judgment in major depression, mania and healthy subjects. A controlled study of 93 subjects. *Acta Psychiatr. Scand.* 109, 222–229. <https://doi.org/10.1046/j.0001-690X.2003.00244.x>
- Buhusi, C. V., Meck, W.H., 2005. What makes us tick? Functional and neural mechanisms of interval timing. *Nat. Rev. Neurosci.* 6, 755–765. <https://doi.org/10.1038/nrn1764>
- Church, R.M., Deluty, M.Z., 1977. Bisection of temporal intervals. *J. Exp. Psychol. Anim. Behav. Process.* 3, 216–228. <https://doi.org/10.1037/0097-7403.3.3.216>
- Church, R.M., 1984. Properties of the internal clock. *Ann. N. Y. Acad. Sci.* 423, 566–582. <https://doi.org/10.1111/j.1749-6632.1984.tb23459.x>
- Corbetta, M., Shulman, G.L., 2011. Spatial neglect and attention networks, *Annual Review of Neuroscience*. <https://doi.org/10.1146/annurev-neuro-061010-113731>

- Craig, A.D., 2009a. Emotional moments across time: A possible neural basis for time perception in the anterior insula. *Philos. Trans. R. Soc. B Biol. Sci.* 364, 1933–1942. <https://doi.org/10.1098/rstb.2009.0008>
- Craig, A.D., 2009b. How do you feel— now? The anterior insula and human awareness. *Nat Rev Neurosci* 10, 59–70. <https://doi.org/10.1038/nrn2555>
- Cromer, J.A., Roy, J.E., Miller, E.K., 2010. Representation of multiple, independent categories in the primate prefrontal cortex. *Neuron* 66, 796–807. <https://doi.org/10.1016/j.neuron.2010.05.005>
- Davalos, D.B., Kiskey, M.A., Ross, R.G., 2002. Deficits in auditory and visual temporal perception in schizophrenia. *Cogn. Neuropsychiatry* 7, 273–282. <https://doi.org/10.1080/13546800143000230>
- Di Lernia, D., Serino, S., Pezzulo, G., Pedroli, E., Cipresso, P., Riva, G., 2018. Feel the time. Time perception as a function of interoceptive processing. *Front. Hum. Neurosci.* 12, 74. <https://doi.org/10.3389/fnhum.2018.00074>
- Eickhoff, S.B., Heim, S., Zilles, K., Amunts, K., 2006. Testing anatomically specified hypotheses in functional imaging using cytoarchitectonic maps. *Neuroimage* 32, 570–582. <https://doi.org/10.1016/j.neuroimage.2006.04.204>
- Eickhoff, S.B., Paus, T., Caspers, S., Grosbras, M.H., Evans, A.C., Zilles, K., Amunts, K., 2007. Assignment of functional activations to probabilistic cytoarchitectonic areas revisited. *Neuroimage* 36, 511–521. <https://doi.org/10.1016/j.neuroimage.2007.03.060>
- Eickhoff, S.B., Stephan, K.E., Mohlberg, H., Grefkes, C., Fink, G.R., Amunts, K., Zilles, K., 2005. A new SPM toolbox for combining probabilistic cytoarchitectonic maps

and functional imaging data. *Neuroimage* 25, 1325–1335.

<https://doi.org/10.1016/j.neuroimage.2004.12.034>

Elsinger, C.L., Harrington, D.L., Rao, S.M., 2006. From preparation to online control:

Reappraisal of neural circuitry mediating internally generated and externally guided actions. *Neuroimage* 31, 1177–1187.

<https://doi.org/10.1016/j.neuroimage.2006.01.041>

Elvevåg, B., McCormack, T., Gilbert, A., Brown, G.D.A., Weinberger, D.R., Goldberg,

T.E., 2003. Duration judgements in patients with schizophrenia. *Psychol. Med.* 33, 1249–1261. <https://doi.org/10.1017/S0033291703008122>

Ferrandez, A.M., Hugueville, L., Lehericy, S., Poline, J.B., Marsault, C., Pouthas, V.,

2003. Basal ganglia and supplementary motor area subtend duration perception: An fMRI study. *Neuroimage* 19, 1532–1544. [https://doi.org/10.1016/S1053-8119\(03\)00159-9](https://doi.org/10.1016/S1053-8119(03)00159-9)

Flandin, G., Friston, K.J., 2019. Analysis of family-wise error rates in statistical

parametric mapping using random field theory. *Hum. Brain Mapp.* 40, 2052–2054. <https://doi.org/10.1002/hbm.23839>

Friston, K.J., Holmes, A., Poline, J. - B., Price, C.J., Frith, C.D., 1996. Detecting

activations in PET and fMRI: levels of inference and power. *Neuroimage* 4, 223–235. <https://doi.org/10.1006/nimg.1996.0074>

Genovesio, A., Tsujimoto, S., Wise, S.P., 2009. Feature- and order-based timing

representations in the frontal cortex. *Neuron* 63, 254–266.

<https://doi.org/10.1016/j.neuron.2009.06.018>

- Genovesio, A., Tsujimoto, S., Wise, S.P., 2011. Prefrontal cortex activity during the discrimination of relative distance. *J. Neurosci.* 31, 3968–3980.
<https://doi.org/10.1523/JNEUROSCI.5373-10.2011>
- Gibbon, J., Church, R.M., Meck, W.H., 1984. Scalar timing in memory. *Ann. N. Y. Acad. Sci.* 423, 52–77. <https://doi.org/10.1111/j.1749-6632.1984.tb23417.x>
- Goodkind, M., Eickhoff, S.B., Oathes, D.J., Jiang, Y., Chang, A., Jones-Hagata, L.B., Ortega, B.N., Zaiko, Y. V., Roach, E.L., Korgaonkar, M.S., Grieve, S.M., Galatzer-Levy, I., Fox, P.T., Etkin, A., 2015. Identification of a common neurobiological substrate for mental illness. *JAMA Psychiatry* 72, 305–315.
<https://doi.org/10.1001/jamapsychiatry.2014.2206>
- Harrington, D.L., Boyd, L.A., Mayer, A.R., Sheltraw, D.M., Lee, R.R., Huang, M., Rao, S.M., 2004a. Neural representation of interval encoding and decision making. *Cogn. Brain Res.* 21, 193–205. <https://doi.org/10.1016/j.cogbrainres.2004.01.010>
- Harrington, D.L., Lee, R.R., Boyd, L.A., Rapcsak, S.Z., Knight, R.T., 2004b. Does the representation of time depend on the cerebellum? Effect of cerebellar stroke. *Brain* 127, 561–574. <https://doi.org/10.1093/brain/awh065>
- Harrington, D.L., Zimbelman, J.L., Hinton, S.C., Rao, S.M., 2010. Neural modulation of temporal encoding, maintenance, and decision processes. *Cereb. Cortex* 20, 1274–1285. <https://doi.org/10.1093/cercor/bhp194>
- Hayashi, M.J., Valli, A., Carlson, S., 2013. Numerical quantity affects time estimation in the suprasecond range. *Neurosci. Lett.* 543, 7–11.
<https://doi.org/10.1016/j.neulet.2013.02.054>

- Hayashi, M.J., van der Zwaag, W., Buetti, D., Kanai, R., 2018. Representations of time in human frontoparietal cortex. *Commun. Biol.* 1, 1–10.
<https://doi.org/10.1038/s42003-018-0243-z>
- Hinton, S.C., Harrington, D.L., Binder, J.R., Durgerian, S., Rao, S.M., 2004. Neural systems supporting timing and chronometric counting: an fMRI study. *Brain Res. Cogn. Brain Res.* 21, 183–192. <https://doi.org/10.1016/j.cogbrainres.2004.04.009>
- Jiang, X., Bradley, E., Rini, R.A., Zeffiro, T., VanMeter, J., Riesenhuber, M., 2007. Categorization training results in shape- and category-selective human neural plasticity. *Neuron* 53, 891–903. <https://doi.org/10.1016/j.neuron.2007.02.015>
- Kopec, C.D., Brody, C.D., 2010. Human performance on the temporal bisection task. *Brain Cogn.* 74, 262–272. <https://doi.org/10.1016/j.bandc.2010.08.006>
- Lane, S.D., Cherek, D.R., Pietras, C.J., Tcheremissine, O. V., 2003. Measurement of delay discounting using trial-by-trial consequences. *Behav. Processes* 64, 287–303. [https://doi.org/10.1016/S0376-6357\(03\)00143-8](https://doi.org/10.1016/S0376-6357(03)00143-8)
- Livesey, A.C., Wall, M.B., Smith, A.T., 2007. Time perception: Manipulation of task difficulty dissociates clock functions from other cognitive demands. *Neuropsychologia* 45, 321–331.
<https://doi.org/10.1016/j.neuropsychologia.2006.06.033>
- Mai, J.K., Majtanik, M., Paxinos, G., 2015. *Atlas of the Human Brain*, 4th ed. Academic Press.
- Meissner, K., Wittmann, M., 2011. Body signals, cardiac awareness, and the perception of time. *Biol. Psychol.* 86, 289–297.
<https://doi.org/10.1016/j.biopsycho.2011.01.001>

- Mella, N., Bourgeois, A., Perren, F., Viaccoz, A., Kliegel, M., Picard, F., 2019. Does the insula contribute to emotion-related distortion of time? A neuropsychological approach. *Hum. Brain Mapp.* 40, 1470–1479. <https://doi.org/10.1002/hbm.24460>
- Mella, N., Conty, L., Pouthas, V., 2011. The role of physiological arousal in time perception: Psychophysiological evidence from an emotion regulation paradigm. *Brain Cogn.* 75, 182–187. <https://doi.org/10.1016/j.bandc.2010.11.012>
- Menon, V., Uddin, L.Q., 2010. Saliency, switching, attention and control: a network model of insula function. *Brain Struct. Funct.* 214, 655–667. <https://doi.org/10.1007/s00429-010-0262-0>
- Monfort, V., Pfeuty, M., Klein, M., Collé, S., Brissart, H., Jonas, J., Maillard, L., 2014. Distortion of time interval reproduction in an epileptic patient with a focal lesion in the right anterior insular/inferior frontal cortices. *Neuropsychologia* 64, 184–194. <https://doi.org/10.1016/j.neuropsychologia.2014.09.004>
- Morita, T., Itakura, S., Saito, D.N., Nakashita, S., Harada, T., Kochiyama, T., Sadato, N., 2008. The Role of the Right Prefrontal Cortex in Self-evaluation of the Face: A Functional Magnetic Resonance Imaging Study. *J. Cogn. Neurosci.* 20, 342–355. <https://doi.org/10.1162/jocn.2008.20.2.342>
- Mottaghy, F.M., Gangitano, M., Krause, B.J., Pascual-Leone, A., 2003. Chronometry of parietal and prefrontal activations in verbal working memory revealed by transcranial magnetic stimulation. *Neuroimage* 18, 565–575. [https://doi.org/10.1016/S1053-8119\(03\)00010-7](https://doi.org/10.1016/S1053-8119(03)00010-7)

- Nagai, M., Kishi, K., Kato, S., 2007. Insular cortex and neuropsychiatric disorders: A review of recent literature. *Eur. Psychiatry* 22, 387–394.
<https://doi.org/10.1016/j.eurpsy.2007.02.006>
- Nakajima, K., Osada, T., Ogawa, A., Tanaka, M., Oka, S., Kamagata, K., Aoki, S., Oshima, Y., Tanaka, S., Konishi, S., 2022. A causal role of anterior prefrontal-putamen circuit for response inhibition revealed by transcranial ultrasound stimulation in humans. *Cell Rep.* 40, 111197.
<https://doi.org/10.1016/j.celrep.2022.111197>
- Nani, A., Manuello, J., Liloia, D., Duca, S., Costa, T., Cauda, F., 2019. The neural correlates of time: A meta-analysis of neuroimaging studies. *J. Cogn. Neurosci.* 31, 1796–1826. https://doi.org/10.1162/jocn_a_01459
- Ogden, R.S., Moore, D., Redfern, L., McGlone, F., 2015. The effect of pain and the anticipation of pain on temporal perception: A role for attention and arousal. *Cogn. Emot.* 29, 910–922. <https://doi.org/10.1080/02699931.2014.954529>
- Oldfield, R.C., 1971. The assessment and analysis of handedness: The Edinburgh inventory. *Neuropsychologia* 9, 97–113. [https://doi.org/10.1016/0028-3932\(71\)90067-4](https://doi.org/10.1016/0028-3932(71)90067-4)
- Plichta, M.M., Vasic, N., Wolf, R.C., Lesch, K.P., Brummer, D., Jacob, C., Fallgatter, A.J., Grön, G., 2009. Neural hyporesponsiveness and hyperresponsiveness during immediate and delayed reward processing in adult attention-deficit/hyperactivity disorder. *Biol. Psychiatry* 65, 7–14.
<https://doi.org/10.1016/j.biopsych.2008.07.008>

- Pollatos, O., Yeldesbay, A., Pikovsky, A., Rosenblum, M., 2014. How much time has passed? Ask your heart. *Front. Neurobot.* 8, 1–9.
<https://doi.org/10.3389/fnbot.2014.00015>
- Pouthas, V., George, N., Poline, J.B., Pfeuty, M., VandeMoorteele, P.F., Hugueville, L., Ferrandez, A.M., Lehericy, S., LeBihan, D., Renault, B., 2005. Neural network involved in time perception: An fMRI study comparing long and short interval estimation. *Hum. Brain Mapp.* 25, 433–441. <https://doi.org/10.1002/hbm.20126>
- Rovelli, C., 2018. *The order of time.* Penguin, London.
- Rubia, K., Halari, R., Christakou, A., Taylor, E., 2009. Impulsiveness as a timing disturbance: neurocognitive abnormalities in attention-deficit hyperactivity disorder during temporal processes and normalization with methylphenidate. *Philos. Trans. R. Soc. B Biol. Sci.* 364, 1919–1931. <https://doi.org/10.1098/rstb.2009.0014>
- Rubia, K., Smith, A., 2004. The neural correlates of cognitive time management: A review. *Acta Neurobiol. Exp. (Wars)*. 64, 329–340.
- Seeley, W.W., 2008. Selective functional, regional, and neuronal vulnerability in frontotemporal dementia. *Curr. Opin. Neurol.* 21, 701–707.
<https://doi.org/10.1097/wco.0b013e3283168e2d>
- Singer, T., Critchley, H.D., Preuschoff, K., 2009. A common role of insula in feelings, empathy and uncertainty. *Trends Cogn. Sci.* 13, 334–340.
<https://doi.org/10.1016/j.tics.2009.05.001>
- Sommer, I.E.C., Diederer, K.M.J., Blom, J.D., Willems, A., Kushan, L., Slotema, K., Boks, M.P.M., Daalman, K., Hoek, H.W., Neggers, S.F.W., Kahn, R.S., 2008.

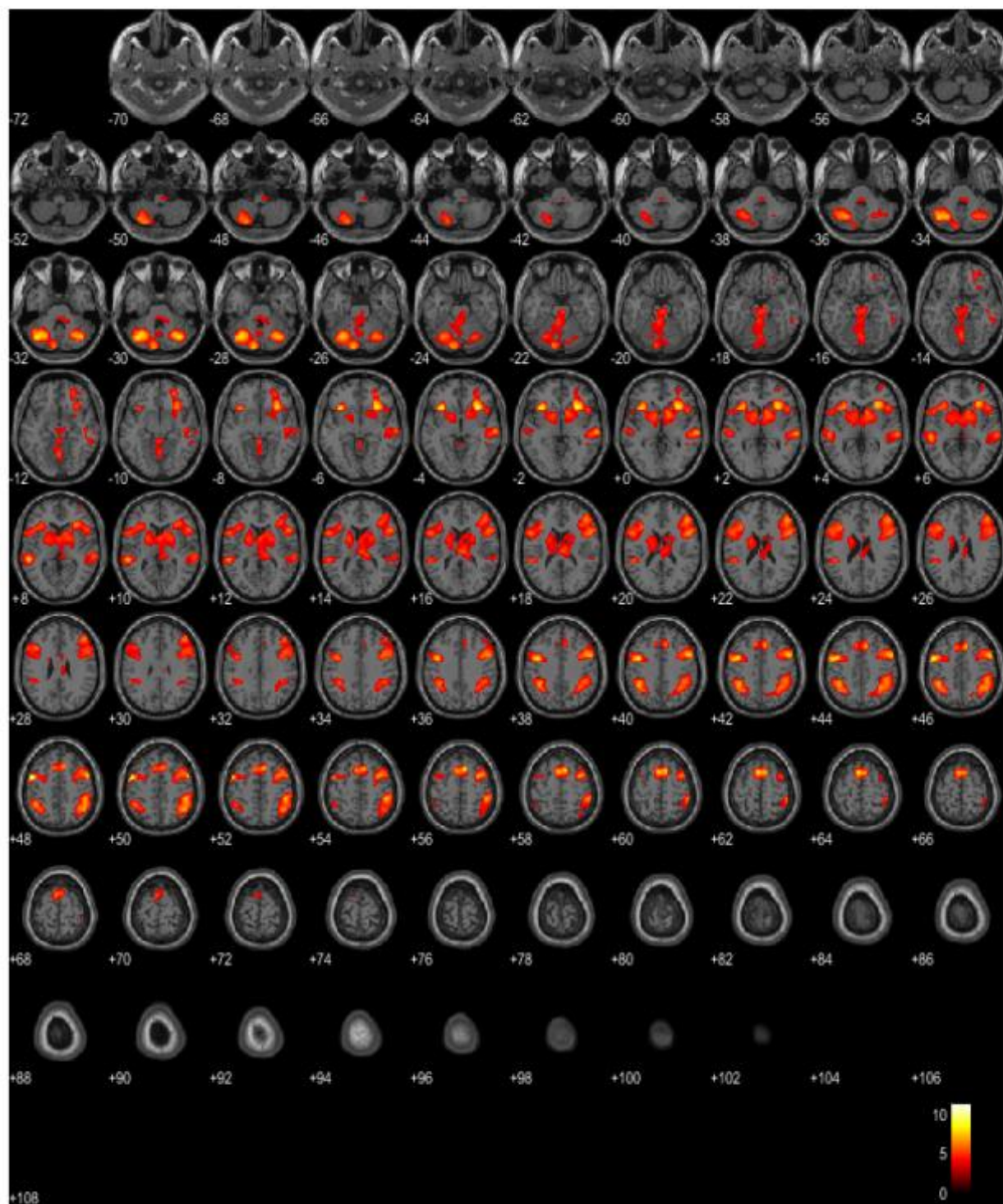
- Auditory verbal hallucinations predominantly activate the right inferior frontal area. *Brain* 131, 3169–3177. <https://doi.org/10.1093/brain/awn251>
- Spagnolo, P.A., Wang, H., Srivanitchapoom, P., Schwandt, M., Heilig, M., Hallett, M., Section, M.C., Medical, P.U., Hospital, S., Neuroscience, A., 2020. HHS Public Access 22, 877–883. <https://doi.org/10.1111/ner.12875>.Lack
- Teghil, A., Boccia, M., D'Antonio, F., Di Vita, A., de Lena, C., Guariglia, C., 2019. Neural substrates of internally-based and externally-cued timing: An activation likelihood estimation (ALE) meta-analysis of fMRI studies. *Neurosci. Biobehav. Rev.* 96, 197–209. <https://doi.org/10.1016/j.neubiorev.2018.10.003>
- Tipples, J., Brattan, V., Johnston, P., 2013. Neural bases for individual differences in the subjective experience of short durations (less than 2 seconds). *PLoS One* 8, e54669. <https://doi.org/10.1371/journal.pone.0054669>
- Treisman, M., Faulkner, A., Naish, P.L., Brogan, D., 1990. The internal clock: evidence for a temporal oscillator underlying time perception with some estimates of its characteristic frequency. *Perception* 19, 705–743. <https://doi.org/10.1068/p190705>
- Unger, R.M., Smolin, L., 2015. *The singular universe and the reality of time*. Cambridge University Press, Cambridge.
- Walsh, V., 2003. A theory of magnitude: Common cortical metrics of time, space and quantity. *Trends Cogn. Sci.* 7, 483–488. <https://doi.org/10.1016/j.tics.2003.09.002>
- Wackermann, J., Späti, J., 2006. Asymmetry of the discrimination function for temporal durations in human subjects. *Acta Neurobiol. Exp. (Wars.)* 66, 245–254.

- Wearden, J.H., 1991. Human Performance on an analogue of an interval bisection task. *Q. J. Exp. Psychol. B.* 43, 59–81.
- Wittmann, M., 2009. The inner experience of time. *Philos. Trans. R. Soc. B Biol. Sci.* 364, 1955–1967. <https://doi.org/10.1098/rstb.2009.0003>
- Wittmann, M., 2013. The inner sense of time: How the brain creates a representation of duration. *Nat. Rev. Neurosci.* 14, 217–223. <https://doi.org/10.1038/nrn3452>
- Wittmann, M., Leland, D.S., Churan, J., Paulus, M.P., 2007. Impaired time perception and motor timing in stimulant-dependent subjects. *Drug Alcohol Depend.* 90, 183–192. <https://doi.org/10.1016/j.drugalcdep.2007.03.005>
- Wittmann, M., Paulus, M.P., 2008. Decision making, impulsivity and time perception. *Trends Cogn. Sci.* 12, 7–12. <https://doi.org/10.1016/j.tics.2007.10.004>
- Wittmann, M., Paulus, M.P., 2009. Temporal horizons in decision making. *J. Neurosci. Psychol. Econ.* 2, 1–11. <https://doi.org/10.1037/a0015460>
- Wittmann, M., Simmons, A.N., Aron, J.L., Paulus, M.P., 2010. Accumulation of neural activity in the posterior insula encodes the passage of time. *Neuropsychologia* 48, 3110–3120. <https://doi.org/10.1016/j.neuropsychologia.2010.06.023>
- Wittmann, M., van Wassenhove, V., 2009. The experience of time: neural mechanisms and the interplay of emotion, cognition and embodiment. *Philos. Trans. R. Soc. B Biol. Sci.* 364, 1809–1813. <https://doi.org/10.1098/rstb.2009.0025>
- Yoshioka, A., Tanabe, H.C., Sumiya, M., Nakagawa, E., Okazaki, S., Koike, T., Sadato, N., 2021. Neural substrates of shared visual experiences: a hyperscanning fMRI study. *Soc. Cogn. Affect. Neurosci.* 28, nsab082. <https://doi.org/10.1093/scan/nsab082>

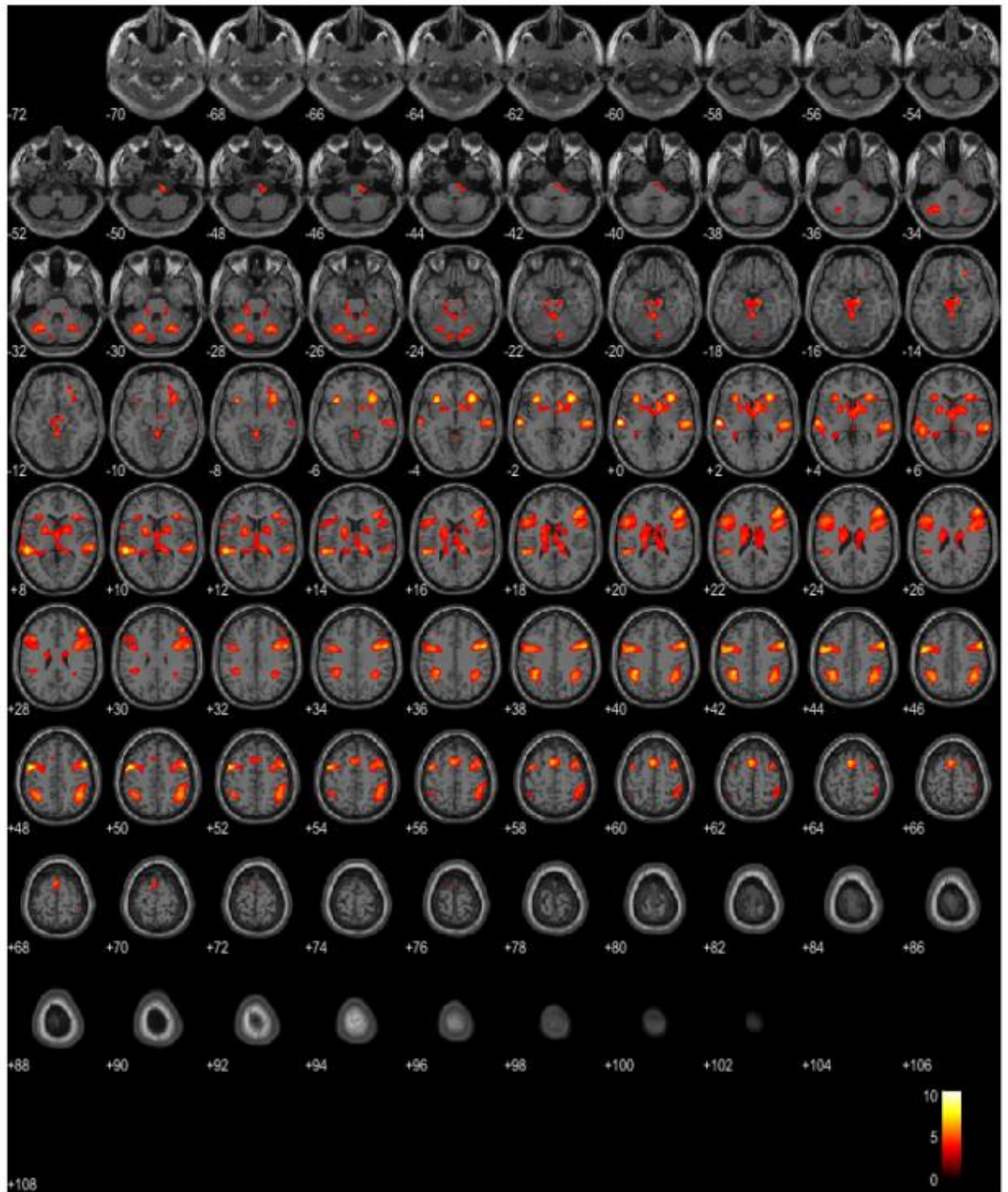
Zhao, W., Li, Y., Du, Y., 2021. TMS Reveals Dynamic Interaction between Inferior Frontal Gyrus and Posterior Middle Temporal Gyrus in Gesture-Speech Semantic Integration. *J. Neurosci.* 41, 10356–10364.
<https://doi.org/10.1523/JNEUROSCI.1355-21.2021>

Zakay, D., Block, R.A., 1997. Temporal cognition. *Curr. Dir. Psychol. Sci.* 6, 12–16.
[https://doi.org/10.1111/1467-8721.ep11512604-dependent subjects](https://doi.org/10.1111/1467-8721.ep11512604-dependent%20subjects). *Drug Alcohol Depend.* 90, 183–192. <https://doi.org/10.1016/j.drugalcdep.2007.03.005>

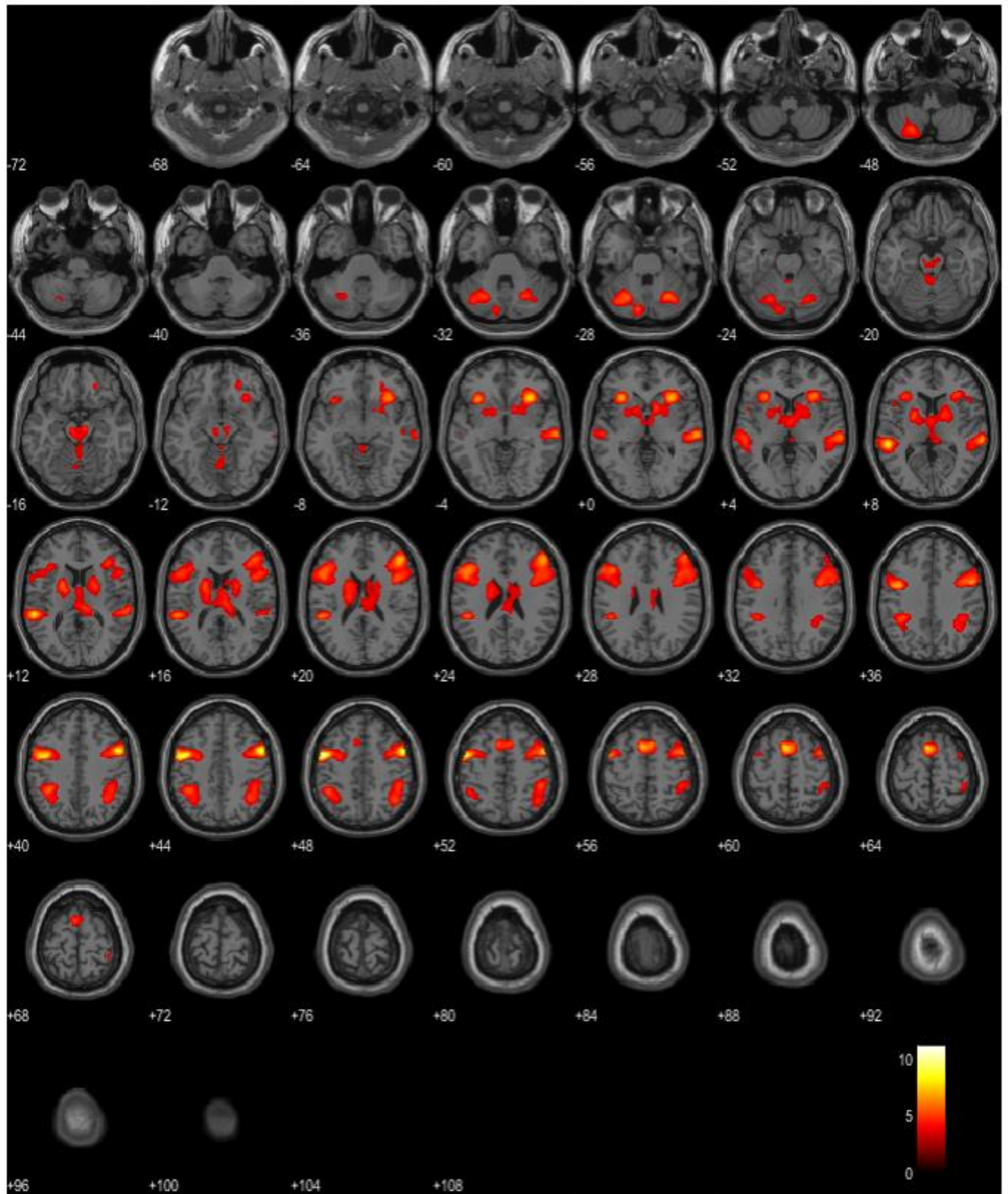
9. Supplementary Figures



Supplementary Figure.1. Axial slice of the areas described by $TB > C$.



Supplementary Figure.2. Axial slices of the area described by $PB > C$.



Supplementary Figure.3. Conjunction between TB > C and PB > C within ANOVA design.

10. Supplementary Tables

Supplementary Table.1.169 trials used in the experiment

Half of the 196 conditions were used as TB and half as PB. The task used as TB by half of the participants was used as PB by the other half of the participants. Conversely, a task used as PB by half of the participants was used as TB by the other half of the participants.

	Task	A1(ms)	A1(Hz)	A2(ms)	A2(Hz)	Target(ms)	Target(Hz)
1	TB (PB)	817	681.4	1762	719.1	817	681.4
2	TB (PB)	1762	681.4	817	719.1	817	681.4
3	TB (PB)	1762	719.1	817	681.4	990	681.4
4	TB (PB)	817	719.1	1762	681.4	990	681.4
5	TB (PB)	817	681.4	1762	719.1	1090	681.4
6	TB (PB)	1762	681.4	817	719.1	1090	681.4
7	TB (PB)	1762	719.1	817	681.4	1200	681.4
8	TB (PB)	817	719.1	1762	681.4	1200	681.4
9	TB (PB)	817	681.4	1762	719.1	1321	681.4
10	TB (PB)	1762	681.4	817	719.1	1321	681.4
11	TB (PB)	1762	719.1	817	681.4	1454	681.4
12	TB (PB)	817	719.1	1762	681.4	1454	681.4
13	TB (PB)	817	681.4	1762	719.1	1762	681.4
14	TB (PB)	1762	681.4	817	719.1	1762	681.4
15	TB (PB)	817	681.4	1762	719.1	817	690.6
16	TB (PB)	1762	681.4	817	719.1	817	690.6
17	TB (PB)	1762	719.1	817	681.4	990	690.6

18	TB (PB)	817	719.1	1762	681.4	990	690.6
19	TB (PB)	817	681.4	1762	719.1	1090	690.6
20	TB (PB)	1762	681.4	817	719.1	1090	690.6
21	TB (PB)	1762	719.1	817	681.4	1200	690.6
22	TB (PB)	817	719.1	1762	681.4	1200	690.6
23	TB (PB)	817	681.4	1762	719.1	1321	690.6
24	TB (PB)	1762	681.4	817	719.1	1321	690.6
25	TB (PB)	1762	719.1	817	681.4	1454	690.6
26	TB (PB)	817	719.1	1762	681.4	1454	690.6
27	TB (PB)	817	681.4	1762	719.1	1762	690.6
28	TB (PB)	1762	681.4	817	719.1	1762	690.6
29	TB (PB)	817	681.4	1762	719.1	817	695.3
30	TB (PB)	1762	681.4	817	719.1	817	695.3
31	TB (PB)	1762	719.1	817	681.4	990	695.3
32	TB (PB)	817	719.1	1762	681.4	990	695.3
33	TB (PB)	817	681.4	1762	719.1	1090	695.3
34	TB (PB)	1762	681.4	817	719.1	1090	695.3
35	TB (PB)	1762	719.1	817	681.4	1200	695.3
36	TB (PB)	817	719.1	1762	681.4	1200	695.3
37	TB (PB)	817	681.4	1762	719.1	1321	695.3
38	TB (PB)	1762	681.4	817	719.1	1321	695.3
39	TB (PB)	1762	719.1	817	681.4	1454	695.3
40	TB (PB)	817	719.1	1762	681.4	1454	695.3

41	TB (PB)	817	681.4	1762	719.1	1762	695.3
42	TB (PB)	1762	681.4	817	719.1	1762	695.3
43	TB (PB)	817	681.4	1762	719.1	817	700
44	TB (PB)	1762	681.4	817	719.1	817	700
45	TB (PB)	1762	719.1	817	681.4	990	700
46	TB (PB)	817	719.1	1762	681.4	990	700
47	TB (PB)	817	681.4	1762	719.1	1090	700
48	TB (PB)	1762	681.4	817	719.1	1090	700
49	TB (PB)	1762	719.1	817	681.4	1200	700
50	TB (PB)	817	719.1	1762	681.4	1200	700
51	TB (PB)	817	681.4	1762	719.1	1321	700
52	TB (PB)	1762	681.4	817	719.1	1321	700
53	TB (PB)	1762	719.1	817	681.4	1454	700
54	TB (PB)	817	719.1	1762	681.4	1454	700
55	TB (PB)	817	681.4	1762	719.1	1762	700
56	TB (PB)	1762	681.4	817	719.1	1762	700
57	TB (PB)	817	681.4	1762	719.1	817	704.7
58	TB (PB)	1762	681.4	817	719.1	817	704.7
59	TB (PB)	1762	719.1	817	681.4	990	704.7
60	TB (PB)	817	719.1	1762	681.4	990	704.7
61	TB (PB)	817	681.4	1762	719.1	1090	704.7
62	TB (PB)	1762	681.4	817	719.1	1090	704.7
63	TB (PB)	1762	719.1	817	681.4	1200	704.7

64	TB (PB)	817	719.1	1762	681.4	1200	704.7
65	TB (PB)	817	681.4	1762	719.1	1321	704.7
66	TB (PB)	1762	681.4	817	719.1	1321	704.7
67	TB (PB)	1762	719.1	817	681.4	1454	704.7
68	TB (PB)	817	719.1	1762	681.4	1454	704.7
69	TB (PB)	817	681.4	1762	719.1	1762	704.7
70	TB (PB)	1762	681.4	817	719.1	1762	704.7
71	TB (PB)	817	681.4	1762	719.1	817	709.5
72	TB (PB)	1762	681.4	817	719.1	817	709.5
73	TB (PB)	1762	719.1	817	681.4	990	709.5
74	TB (PB)	817	719.1	1762	681.4	990	709.5
75	TB (PB)	817	681.4	1762	719.1	1090	709.5
76	TB (PB)	1762	681.4	817	719.1	1090	709.5
77	TB (PB)	1762	719.1	817	681.4	1200	709.5
78	TB (PB)	817	719.1	1762	681.4	1200	709.5
79	TB (PB)	817	681.4	1762	719.1	1321	709.5
80	TB (PB)	1762	681.4	817	719.1	1321	709.5
81	TB (PB)	1762	719.1	817	681.4	1454	709.5
82	TB (PB)	817	719.1	1762	681.4	1454	709.5
83	TB (PB)	817	681.4	1762	719.1	1762	709.5
84	TB (PB)	1762	681.4	817	719.1	1762	709.5
85	TB (PB)	817	681.4	1762	719.1	817	719.1
86	TB (PB)	1762	681.4	817	719.1	817	719.1

87	TB (PB)	1762	719.1	817	681.4	990	719.1
88	TB (PB)	817	719.1	1762	681.4	990	719.1
89	TB (PB)	817	681.4	1762	719.1	1090	719.1
90	TB (PB)	1762	681.4	817	719.1	1090	719.1
91	TB (PB)	1762	719.1	817	681.4	1200	719.1
92	TB (PB)	817	719.1	1762	681.4	1200	719.1
93	TB (PB)	817	681.4	1762	719.1	1321	719.1
94	TB (PB)	1762	681.4	817	719.1	1321	719.1
95	TB (PB)	1762	719.1	817	681.4	1454	719.1
96	TB (PB)	817	719.1	1762	681.4	1454	719.1
97	TB (PB)	817	681.4	1762	719.1	1762	719.1
98	TB (PB)	1762	681.4	817	719.1	1762	719.1
99	PB(TB)	1762	719.1	817	681.4	817	681.4
100	PB(TB)	817	719.1	1762	681.4	817	681.4
101	PB(TB)	817	681.4	1762	719.1	990	681.4
102	PB(TB)	1762	681.4	817	719.1	990	681.4
103	PB(TB)	1762	719.1	817	681.4	1090	681.4
104	PB(TB)	817	719.1	1762	681.4	1090	681.4
105	PB(TB)	817	681.4	1762	719.1	1200	681.4
106	PB(TB)	1762	681.4	817	719.1	1200	681.4
107	PB(TB)	1762	719.1	817	681.4	1321	681.4
108	PB(TB)	817	719.1	1762	681.4	1321	681.4
109	PB(TB)	817	681.4	1762	719.1	1454	681.4

110	PB(TB)	1762	681.4	817	719.1	1454	681.4
111	PB(TB)	1762	719.1	817	681.4	1762	681.4
112	PB(TB)	817	719.1	1762	681.4	1762	681.4
113	PB(TB)	1762	719.1	817	681.4	817	690.6
114	PB(TB)	817	719.1	1762	681.4	817	690.6
115	PB(TB)	817	681.4	1762	719.1	990	690.6
116	PB(TB)	1762	681.4	817	719.1	990	690.6
117	PB(TB)	1762	719.1	817	681.4	1090	690.6
118	PB(TB)	817	719.1	1762	681.4	1090	690.6
119	PB(TB)	817	681.4	1762	719.1	1200	690.6
120	PB(TB)	1762	681.4	817	719.1	1200	690.6
121	PB(TB)	1762	719.1	817	681.4	1321	690.6
122	PB(TB)	817	719.1	1762	681.4	1321	690.6
123	PB(TB)	817	681.4	1762	719.1	1454	690.6
124	PB(TB)	1762	681.4	817	719.1	1454	690.6
125	PB(TB)	1762	719.1	817	681.4	1762	690.6
126	PB(TB)	817	719.1	1762	681.4	1762	690.6
127	PB(TB)	1762	719.1	817	681.4	817	695.3
128	PB(TB)	817	719.1	1762	681.4	817	695.3
129	PB(TB)	817	681.4	1762	719.1	990	695.3
130	PB(TB)	1762	681.4	817	719.1	990	695.3
131	PB(TB)	1762	719.1	817	681.4	1090	695.3
132	PB(TB)	817	719.1	1762	681.4	1090	695.3

133	PB(TB)	817	681.4	1762	719.1	1200	695.3
134	PB(TB)	1762	681.4	817	719.1	1200	695.3
135	PB(TB)	1762	719.1	817	681.4	1321	695.3
136	PB(TB)	817	719.1	1762	681.4	1321	695.3
137	PB(TB)	817	681.4	1762	719.1	1454	695.3
138	PB(TB)	1762	681.4	817	719.1	1454	695.3
139	PB(TB)	1762	719.1	817	681.4	1762	695.3
140	PB(TB)	817	719.1	1762	681.4	1762	695.3
141	PB(TB)	1762	719.1	817	681.4	817	700
142	PB(TB)	817	719.1	1762	681.4	817	700
143	PB(TB)	817	681.4	1762	719.1	990	700
144	PB(TB)	1762	681.4	817	719.1	990	700
145	PB(TB)	1762	719.1	817	681.4	1090	700
146	PB(TB)	817	719.1	1762	681.4	1090	700
147	PB(TB)	817	681.4	1762	719.1	1200	700
148	PB(TB)	1762	681.4	817	719.1	1200	700
149	PB(TB)	1762	719.1	817	681.4	1321	700
150	PB(TB)	817	719.1	1762	681.4	1321	700
151	PB(TB)	817	681.4	1762	719.1	1454	700
152	PB(TB)	1762	681.4	817	719.1	1454	700
153	PB(TB)	1762	719.1	817	681.4	1762	700
154	PB(TB)	817	719.1	1762	681.4	1762	700
155	PB(TB)	1762	719.1	817	681.4	817	704.7

156	PB(TB)	817	719.1	1762	681.4	817	704.7
157	PB(TB)	817	681.4	1762	719.1	990	704.7
158	PB(TB)	1762	681.4	817	719.1	990	704.7
159	PB(TB)	1762	719.1	817	681.4	1090	704.7
160	PB(TB)	817	719.1	1762	681.4	1090	704.7
161	PB(TB)	817	681.4	1762	719.1	1200	704.7
162	PB(TB)	1762	681.4	817	719.1	1200	704.7
163	PB(TB)	1762	719.1	817	681.4	1321	704.7
164	PB(TB)	817	719.1	1762	681.4	1321	704.7
165	PB(TB)	817	681.4	1762	719.1	1454	704.7
166	PB(TB)	1762	681.4	817	719.1	1454	704.7
167	PB(TB)	1762	719.1	817	681.4	1762	704.7
168	PB(TB)	817	719.1	1762	681.4	1762	704.7
169	PB(TB)	1762	719.1	817	681.4	817	709.5
170	PB(TB)	817	719.1	1762	681.4	817	709.5
171	PB(TB)	817	681.4	1762	719.1	990	709.5
172	PB(TB)	1762	681.4	817	719.1	990	709.5
173	PB(TB)	1762	719.1	817	681.4	1090	709.5
174	PB(TB)	817	719.1	1762	681.4	1090	709.5
175	PB(TB)	817	681.4	1762	719.1	1200	709.5
176	PB(TB)	1762	681.4	817	719.1	1200	709.5
177	PB(TB)	1762	719.1	817	681.4	1321	709.5
178	PB(TB)	817	719.1	1762	681.4	1321	709.5

179	PB(TB)	817	681.4	1762	719.1	1454	709.5
180	PB(TB)	1762	681.4	817	719.1	1454	709.5
181	PB(TB)	1762	719.1	817	681.4	1762	709.5
182	PB(TB)	817	719.1	1762	681.4	1762	709.5
183	PB(TB)	1762	719.1	817	681.4	817	719.1
184	PB(TB)	817	719.1	1762	681.4	817	719.1
185	PB(TB)	817	681.4	1762	719.1	990	719.1
186	PB(TB)	1762	681.4	817	719.1	990	719.1
187	PB(TB)	1762	719.1	817	681.4	1090	719.1
188	PB(TB)	817	719.1	1762	681.4	1090	719.1
189	PB(TB)	817	681.4	1762	719.1	1200	719.1
190	PB(TB)	1762	681.4	817	719.1	1200	719.1
191	PB(TB)	1762	719.1	817	681.4	1321	719.1
192	PB(TB)	817	719.1	1762	681.4	1321	719.1
193	PB(TB)	817	681.4	1762	719.1	1454	719.1
194	PB(TB)	1762	681.4	817	719.1	1454	719.1
195	PB(TB)	1762	719.1	817	681.4	1762	719.1
196	PB(TB)	817	719.1	1762	681.4	1762	719.1

Supplementary Table.2. Neural activation during TB contrasted with PB masked by

TB > C.

The statistical threshold was set at $p < .05$, and FWE was corrected at the cluster level using the height threshold of uncorrected $p < .001$. TB, temporal bisection task; PB, pitch bisection task; C, control task; Hem, Hemisphere; R, right; L, left. IFG, inferior frontal gyrus; IPL, inferior parietal lobule; SMG, supramarginal gyrus; MCC, midcingulate cortex; MFG, middle frontal gyrus. Location was identified with the SPM Anatomy toolbox Version 2.2b.

Spatial extent test	cluster	MNI coordinates			T value	Hem	Anatomical Location	probability
Cluster size(mm3)	p(FWE-corr)	x	y	z				
5824	<0.001	54	18	2	6.94	R	IFG(p. Opercularis)	28.6
		50	20	0	6.93	R	IFG (p. Triangularis)	35.6
		36	20	2	5.71	R	Insula	
2808	0.003	54	-42	34	6.27	R	SMG	PFm (IPL) 37.2
		56	-36	56	4.80	R	IPL	PFt (IPL) 10.4
		52	-36	46	4.45	R	IPL	hIP2 (IPS) 30.7
4000	<0.001	-30	-72	-34	6.04	L	Cerebellum	Lobule VIIa crusI (Hem) 38
		-22	-76	-42	4.27	L	Cerebellum	Lobule VIIa crusII (Hem) 52
		-46	-54	-32	3.94	L	Cerebellum	Lobule VIIa crusI (Hem) 100
2384	0.006	6	36	38	5.22	R	Superior Medial Gyrus	
		6	34	42	4.95	R	Superior Medial Gyrus	
		8	22	56	4.33	R	Posterior-Medial Frontal	
		10	18	58	4.20	R	Posterior-Medial Frontal	
		8	32	32	4.07	R	MCC	
		6	14	66	3.98	R	Posterior-Medial Frontal	
		-10	14	48	3.68	L	Posterior-Medial Frontal	
1504	0.027	-2	18	44	3.57	L	Posterior-Medial Frontal	
		36	-56	-32	5.16	R	Cerebellum	Lobule VIIa crusI (Hem) 75.2
		46	-60	-34	5.10	R	Cerebellum	Lobule VIIa crusI (Hem) 97.2
1512	0.026	42	12	46	5.06	R	MFG	
		32	10	50	3.78	R	MFG	

Supplementary Table.3. Inter-individual covariation with TB-specific activation (TB > PB) with BP masked by TB > C.

The statistical threshold was set at $p < .05$, FWE corrected at cluster level using the height threshold of uncorrected $p < .001$, within the volume defined by TB > C. TB, temporal bisection task; PB, pitch bisection task; C, control task; Hem, Hemisphere; R, right; L, left. IFG, inferior frontal gyrus. Location was identified with the SPM Anatomy toolbox

Version 2.2b.

Spatial extent test	cluster	MNI coordinates			T value	Hem	Anatomical Location	probability
Cluster size(mm3)	p(FWE-corr)	x	y	z				
1304	0.017	34	16	-8	5.56	R	Insula	
1720	0.007	48	24	14	5.22	R	IFG (p. Triangularis)	16.2
		56	16	10	4.30	R	IFG (p. Opercularis)	46.4
		54	8	10	4.19	R	IFG (p. Opercularis)	64

Supplementary Table.4. Neural substrates activation during TB contrasted with C.

The statistical threshold was set at $p < .05$, and FWE was corrected at cluster level using the height threshold of uncorrected $p < .001$, across the whole brain. TB, temporal bisection task; C, control task; Hem, Hemisphere; R, right; L, left. SMG, supramarginal gyrus; IPL, inferior parietal lobule; MTG, middle temporal gyrus; STG, superior temporal gyrus.

Location was identified with the SPM Anatomy toolbox Version 2.2b.

Spatial extent test	cluster	MNI coordinates			T value	Hem	Anatomical Location	probability
Cluster size(mm3)	p(FWE-corr)	x	y	z				
121288	<0.001	-48	2	48	11.32	L	Precentral Gyrus	
		-42	0	42	9.42	L	Precentral Gyrus	
		30	20	-4	9.25	R		
13592	<0.001	-4	12	62	8.99	L	Posterior-Medial Frontal	
		8	16	58	8.81	R	Posterior-Medial Frontal	
		10	22	44	7.71	R	SMG	
46880	<0.001	38	-68	-30	8.49	R	Cerebellum	VIIa crusI (Hem) 100.0
		-36	-68	-30	8.32	L	Cerebellum	VIIa crusI (Hem) 100
		28	-66	-30	7.65	R	Cerebellum	VI (Hem) 52.8
18288	<0.001	-38	-46	40	7.95	L	IPL	hIP1 (IPS) 39
		-54	-36	8	7.87	L	MTG	
		-38	-56	42	6.37	L	IPL	hIP1 (IPS) 61.4
21152	<0.001	48	-36	52	7.64	R	IPL	Area2 18.1
		44	-56	50	7.23	R	IPL	PGa (IPL) 30.4
		36	-52	44	7.05	R	IPL	hIP3 (IPS) 47.8
11240	<0.001	66	-24	0	7.51	R	STG	TE 3 53.1
		50	-20	-8	5.06	R	MTG	
		50	-34	12	4.83	R	STG	PFcm (IPL) 30.4

Supplementary Table.5. Neural substrates activation during PB contrasted with C.

The statistical threshold was set at $p < .05$, and FWE was corrected at cluster level using the height threshold of uncorrected $p < .001$, across the whole brain. PB, temporal bisection task; C, control task; Hem, Hemisphere; R, right; L, left; IPL, inferior parietal lobule; STG, superior temporal gyrus; PMF, posterior medial frontal. Location was identified with the

SPM Anatomy toolbox Version 2.2b.

Spatial extent test	cluster	MNI coordinates			T value	Hem	Anatomical Location	probability
Cluster size(mm3)	p(FWE-corr)	x	y	z				
119848	<0.001	-60	-22	2	10.552	L	Superior Temporal Gyrus(STG) TE3	2.2
		-56	-36	10	9.357	L	Superior Temporal Gyrus(STG)	8.2
		30	22	-2	9.245			
7656	<0.001	60	-22	0	7.759	R	Superior Temporal Gyrus(STG)	
		64	-28	6	6.587	R	Superior Temporal Gyrus(STG) TE3	43.1
		46	-34	12	5.030	R	Superior Temporal Gyrus(STG) PFcm(IPL)	32.6
5240	0.001	-4	10	62	7.377	L	Posterior-Medial Frontal(PMF)	
		-8	2	76	3.553	L	Posterior-Medial Frontal(PMF)	
14240	<0.001	40	-48	46	6.872	R	Inferior Parietal Lobule(IPL) hIP3 (IPS)	34
		34	-56	42	6.170	R	Angular Gyrus hIP1 (IPS)	12.7
4864	0.001	26	-66	-28	6.213	R	Cerebellum (VI) VI (Hem)	86
		34	-68	-28	5.389	R	Cerebellum (Crus 1) VIIa crusI (Hem)	82.4
		-10	-80	-26	5.081	L	Cerebellum (Crus 1) VIIa crusI (Hem)	62.8
4048	0.004	-26	-64	-30	5.873	L	Cerebellum (VI) VI (Hem)	70.4
		-38	-70	-30	5.239	L	Cerebellum (Crus 1) VIIa crusI (Hem)	98.8
2392	0.037	12	-22	-50	5.627			
		16	-36	-28	3.959	R	Cerebellum (III) I IV (Hem)	85.6
		18	-28	-32	3.951		I IV (Hem)	7.2